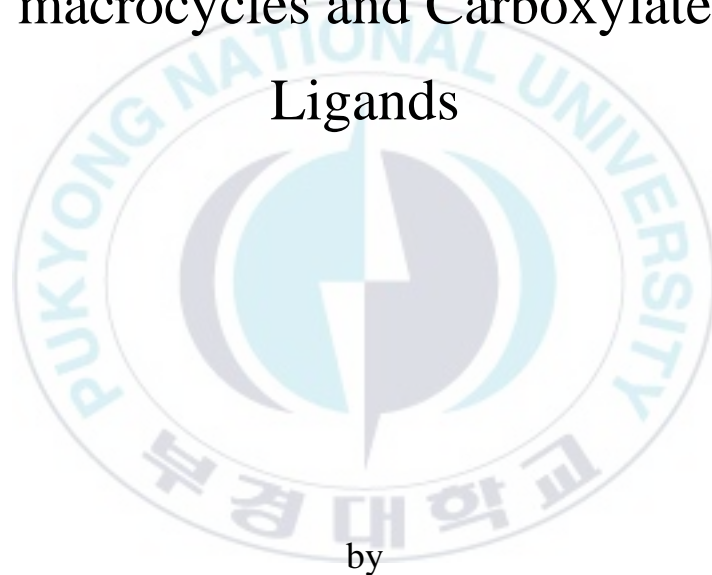Thesis for the Degree

Master of Education

Studies of Coordination Polymers constructed from Zn(II), Ni(II) macrocycles and Carboxylate Ligands

by

Han Young Park

Graduate School of Education

Pukyong National University

August 2007

Studies of Coordination Polymers constructed from Zn(II), Ni(II) macrocycles and Carboxylate Ligands

니켈(II) 및 아연(II) 거대고리 착화합물과 카복실산 리간드를 이용한 배위고분자 화합물에 관한 연구

Advisor : Prof. Ju Chang Kim

by

Han Young Park

A thesis submitted in partial fulfillment of the requirement
for the degree of
Master of Education

Graduate School of Education
Pukyong National University

August 2007

Studies of Coordination Polymers constructed from Zn(II), Ni(II) macrocycles and Carboxylate Ligands

A dissertation

by
Han Young Park

Approved by :

_____
Chairman: Sang Yong Pyun

_____   _____

Member: Yong-Cheol Kang   Member: Ju Chang Kim

August 30, 2007

Table of Contents

CHAPTER III. One-dimensional macrocyclic zinc(II) coordination polymers containing an unusual coordination of polycarboxylate ligands

List of Tables

List of Figures

Studies of Coordination Polymers constructed from Zn(II), Ni(II)

macrocycles and Carboxylate Ligands

박 한 영

부경대학교 교육대학원 화학교육전공

요 약

$\{[Zn(\textbf{L1})(maleate)] \cdot H_2O\}_n$, $[Zn(\textbf{L1})(H_2O)_2](fumarate) \cdot 4H_2O$, $[Ni(\textbf{L1})(Hdipic)_2] \cdot 2H_2O$, $[Ni(\textbf{L1})(H_2O)_2][Ni(dipic)_2] \cdot 2.5H_2O$, $\{[Zn(\textbf{L2})(oxalate)] \cdot 3.5H_2O\}_n$, $\{[Zn(\textbf{L2})(H_2pm)] \cdot H_2O\}_n$ (**L1** = 1,4,8,11-tetraazacyclotetradecane, cyclam, **L2** = 5,16-dimethyl-2,6,13,17-tetraazatricyclo$[16.4.0^{1,18}.0^{7,12}]$docosane, dipic = 2,6-pyridinedicarboxylate, dipicolinate, pm = 1,2,4,5-benzenetetracarboxylate, pyromellitate)의 조성을 갖는 6개의 새로운 화합물을 합성하였고, 원소분석, 분광학 및 결정학적 방법을 통하여 그 구조적 특성을 확인 하였다. 이 화합물들은 대부분 금속 이온 거대고리 착화합물과 카복실산 음이온 다리 리간드의 공유결합 및 수소결합을 통한 1D 고분자 사슬 구조를 형성하였고, 3D 초분자나 단분자 구조, 또는 molecular salt를 형성하기도 하였다. 모든 착화합물 들에서 다양한 형태의 수소결합 상호작용과 거대고리 리간드의 미리 자리잡고있 는 N-H의 방향성이 카복실산 음이온 리간드의 형태 결정뿐 아니라 금속과 리간드 간의 결합을 강화하는데 중요한 역할을 하였다. 방향족 카복실산 리간드(2,6-pyridinedicarboxylate, 1,2,4,5-benzenetetracarboxylate)를 이용한 화합물 $[Ni(\textbf{L1})(Hdipic)_2] \cdot 2H_2O$와 $\{[Zn(\textbf{L2})(H_2pm)] \cdot H_2O\}_n$에서는 1D 배위고분자 화합물을 형 성함에 있어 수소결합 상호작용 외에 $\pi\text{-}\pi$ stacking 상호작용 또한 중요한 원동력으 로 작용하였다. 마지막으로 거대고리 리간드 **L2**를 이용한 화합물 $\{[Zn(\textbf{L2})(oxalate)] \cdot 3.5H_2O\}_n$과 $\{[Zn(\textbf{L2})(H_2pm)] \cdot H_2O\}_n$은 다리 리간드들이 독특한 배 위양상을 보이며, 1D 고분자 사슬 구조를 형성하고 있었다. 거대고리 리간드 **L2**의 경직성과 입체 장애가 이 독특한 배위양상을 나타내게 하는 중요한 요인임을 알 수 있었다.

General Introduction

Coordination polymers are metal-ligand compounds that are composed of metal ion 'connectors' and bridging ligand 'linkers', and they can extend infinitely into one, two or three dimensional structures [1,3]. Weaker noncovalent interactions such as hydrogen bonds or π-π stacks also play an important role during the construction of coordination polymers [3].

The applications of coordination polymers are widely spread in the areas of catalysis, chirality, conductivity, luminescence, magnetism, spin-transition (spin-crossover), non-linear optics (NLO), and gas storage [2,3].

The important characteristics of metal ion 'connectors' are the number and orientation of their binding sites (coordination numbers and coordination geometries). Depending on the metal ions and their oxidation states, the coordination numbers can be ranged from 2 to 7, giving rise to various geometries, which can be linear, tetrahedral, square-planar, square-pyramidal, trigonal-bipyramidal, octahedral, trigonal-prismatic, pentagonal-bipyramidal, and the corresponding distorted forms [1].

The ligands as 'linkers' afford a wide variety of linking sites with various binding strength and directionality. Therefore, the dimensionalities of

coordination polymers can be tuned by carefully selecting organic ligands. The bridging ligands commonly used in the construction of coordination polymers are 4,4'-bipyridine, 1,4-diaza-bicyclo[2.2.2]octane, pyrazine, oxalate, terephthalate, benzenetricarboxylate, and benzenetetracarboxylate, etc. [1~3]

Polyazamacrocyclic complexes with multi-connecting ligands have been proved to be good building blocks for the construction of coordination polymers. So, we have used metallotetraazamacrocycles and several bridging ligands as building blocks to construct coordination polymers and to investigate intermolecular interactions that have an effect on their structures and properties. Metallotetraazamacrocycles have been reported to be good 'connectors' because the axial sites of the metal ions are opened for incoming bridging ligands 'linkers' [4].

The bridging ligand is one of the important factors that influence the whole structures of the coordination polymers. Multidentate polycarboxylate anions are well-known versatile ligands that are able to chelate and bridge metal ions for the formation of polynuclear systems. And they can act not only as hydrogen bond donors but also hydrogen bond acceptors due to the existence of protonated and/or deprotonated carboxyl groups [5,6].

On the basis of the aforementioned points, we have attempted to construct

coordination polymers with tetraazamacrocyclic ligands and polycarboxylate ligands. In this thesis, the syntheses and properties of new macrocyclic Zn(II) and Ni(II) carboxylato complexes have been described, where each metallotetraazamacrocycle is bridged by polycarboxylates such as maleate, 2,6-pyridinedicarboxylate, 1,2,4,5-benzenetetracarboxylate, and oxalate anions. In all complexes, various types of hydrogen bonding interactions and the pre-organization of N-H groups play an important role in reinforcing the metal-ligand ligations as well as in determining the shapes of the carboxylate anions. The π-π stacking interactions were observed in several complexes, too. The details of the structures for the new complexes were determined by analytical, spectroscopic, and X-ray diffraction methods.

Overall, this thesis is composed of three chapters. In the Chapter I, the syntheses and properties of two novel Zn(II) complexes with tetraazamacrocyclic ligand are reported. The maleate and isomeric fumarate anions show the different molecular interactions with Zn(II) macrocycle.

In the Chapter II, the syntheses and properties of two new Ni(II) complexes are reported. These new complexes indicate the different coordination modes of Hdipic and dipic ligands to Ni(II) ions in a same environment.

In the Chapter III, the syntheses and structures of new one-dimensional

coordination polymers are described. These 1D polymers are built by taking advantage of the rigidity, directionality and steric hindrance of the Zn(II) macrocycle 'connectors' along with the ability of oxalate and 1,2,4,5-benzenetetracarboxylate 'linkers' to bridge between Zn(II) ions.

References

[1]   S. Kitagawa, R. Kitaura, S. Noro, Angew. Chem. Int. Ed. 43 (2004) 2334.

[2]   Y.Y. Yang, W.T. Wong, Chem. Commun. 22 (2002) 2716.

[3]   C. Janiak, Dalton Trans. 19 (2003) 2781.

[4]   H. Park, J.C. Kim, A.J. Lough, B.M. Lee, Inorg. Chem. Commun. 10 (2007) 303.

[5]   H. Park, M.H. Jeong, J.C. Kim, A.J. Lough, Bull. Korean Chem. Soc. 28 (2007)

[6]   Y. Li, N. Hao, Y. Lu, E. Wang, Z. Kang, C. Hu, Inorg. Chem. 42 (2003) 3119.

CHAPTER I

Molecular interactions of zinc(II) cyclams toward maleate and fumarate anions

Abstract

Two new zinc(II) complexes of the composition $\{[Zn(\mathbf{L1})(maleate)]\cdot H_2O\}_n$ (**1**) and $[Zn(\mathbf{L1})(H_2O)_2](fumarate)\cdot 4H_2O$ (**2**) (**L1** = cyclam, 1,4,8,11-tetraazacyclotetradecane) have been prepared and structurally characterized by a combination of analytical, spectroscopic, thermogravimetric, and crystallographic methods. The carboxylate groups of the maleate ligand in **1** show a coordination tendency toward zinc(II) cyclams resulting in the formation of a 1D coordination polymer. However, the carboxylate groups of the isomeric fumarate anion in **2** do not interact with zinc(II) cyclam. The identification of strong interactions between carboxylate groups and zinc(II) ions in **1** may provide better knowledge for the improved design of receptor-targeted zinc(II) cyclams in anti-HIV agents.

Introduction

Cyclams and bicyclams attract increasing interests owing to their highly potent and selective anti-HIV activity by specifically blocking the co-receptor CXCR4 [1-3]. Particularly, the Xylyl-bicyclam AMD3100 ([1,1'-(1,4-phenylenebismethylene)-bis-1,4,8,11-tetraazacyclotetradecane·8HCl·2H$_2$O]) has recently been on clinical trials for the treatment of AIDS, and stem cell plantation for the treatment of patients who have cancers involving the blood and immune system [4-6]. Cyclam itself is known to exhibit significant anti-HIV activity as well. It has been suggested that aspartate residues having carboxylate groups (Asp 171 and Asp 262) of the CXCR4 co-receptor play key roles in the recognition of cyclams [1,7]. It is also understood that the metal complexation, especially the zinc(II) ion complexation to cyclams and bicyclams greatly enhance the antiviral activity than free ligands [3]. Therefore, the knowledge of interactions between carboxylates and zinc(II) cyclams is important in the design and development of more effective anti-HIV agents. In this chapter, several zinc(II) complexes have been prepared and structurally characterized in order to elucidate a selective recognition of zinc(II) cyclams by carboxylates [6,8,9]. Nevertheless, the examples of

carboxylato zinc(II) cyclams are still rare. As a continuation of our investigations on expanding such complexes and understanding the nature of interactions between zinc(II) cyclams and carboxylates, we attempted reactions between [Zn(**L1**)][ClO$_4$]$_2$ and sodium maleate (two carboxylate groups are mutually *cis* through the carbon-carbon double bond) or sodium fumarate (two carboxylate groups are mutually *trans* through the carbon-carbon double bond). In this chapter, I describe the synthesis, structures and properties of new zinc(II) complexes **1** and **2**.
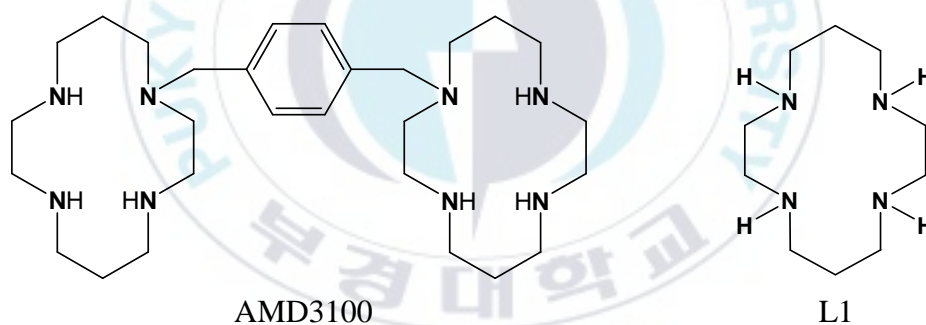
AMD3100   L1

Experimental

Materials and Methods

All chemicals used in the synthesis were reagent grade and were used without further purification. Distilled water was used for all procedures. Infrared spectra of solid samples were recorded in a Perkin-Elmer Paragon 1000 FT-IR spectrophotometer between 4000cm^{-1} and 400cm^{-1} as Nujol mulls on KBr discs. Thermal analysis (TGA-DTG) was performed on a Perkin-Elmer Model TGA-7 Thermogravimetric Analyzer under air from 50 to 800 ^{o}C at a heating rate of 10 ^{o}C/min. Elemental analysis was performed by the Korea Research Institute of Chemical Technology, Daejeon, Korea. The precursor complex [Zn(**L1**)][ClO$_4$]$_2$ was prepared according to the literature procedures previously reported [8].

Caution! Perchlorate salts of metal complexes with organic ligands are potentially explosive. Only small amounts of the materials should be prepared, and these should be handled with care.

Synthesis of 1

To a DMF (N,N-dimethylformamide) solution (10ml) of [Zn(**L1**)][ClO$_4$]$_2$ (232 mg, 0.5 mmol) was added an aqueous solution (10ml) of sodium maleate (80 mg, 0.5 mmol) in an open beaker. Colorless single crystals of **1** were obtained in a week. The complex **1** was stable indefinitely in the air. Suitable crystals of **1** for X-ray diffraction studies and subsequent spectroscopic measurements were manually collected under a microscope. Anal. Calcd. for C$_{14}$H$_{28}$N$_4$O$_5$Zn (**1**): C, 42.24; N, 14.08; H, 7.04%. Found: C, 42.22; N, 13.96; H, 7.37%.

Synthesis of 2

To a DMF solution (10ml) of [Zn(**L1**)][ClO$_4$]$_2$ (232 mg, 0.5 mmol) was added an aqueous solution (10ml) of sodium fumarate (80 mg, 0.5 mmol). Colorless single crystals of **2** were obtained in a week. The complex **2** retained its transparency for several weeks with mother liquor in a refrigerator, but it lost solvent water molecules in several days upon exposure to atmosphere as evidenced by thermal analysis. Suitable crystals of **2** for X-ray diffraction

studies and subsequent spectroscopic measurements were manually collected under the microscope. Anal. Calcd. for $C_{14}H_{38}N_4O_{10}Zn$ (**2**): C, 34.44; N, 11.48; H, 7.79%. Found: C, 34.29; N, 11.28; H, 7.47%.

X-ray crystallography

A summary of selected crystallographic data for **1** and **2** are given in Table 1.1. The data were collected on a Nonius Kappa CCD diffractometer, using graphite monochromated Mo K_α radiation ($\lambda = 0.71073$ Å). A combination of 1° ϕ and ω (with κ offsets) scans were used to collect sufficient data. The data frames were integrated and scaled using the Denzo-SMN package [10]. The structure was solved and refined, using the SHELXTL\PC V5.1 package [11]. Refinement was performed by full-matrix least squares on F^2 using all data (negative intensities included). Hydrogen atoms were included in calculated positions, except for those involving hydrogen bonding specifically for the hydrogen atoms bonded to the nitrogen atoms, which were refined with isotropic thermal parameters.

Table 1.1. Crystal data and structure refinement for {[Zn(**L1**)(maleate)]·H_2O}$_n$
(**1**) and [Zn(**L1**)(H_2O)$_2$](fumarate)·4H_2O(**2**)

	1	2
Empirical formula	$C_{14}H_{28}N_4O_5Zn$	$C_{14}H_{38}N_4O_{10}Zn$
Formula weight	397.77	487.85
Temperature (K)	150(2)	150(2)
Crystal system	Monoclinic	Triclinic
Space group	P 2$_1$/n	P -1
a (Å)	15.1376(4)	7.0809(2)
b (Å)	8.3063(4)	8.8867(3)
c (Å)	15.3944(6)	9.3322(2)
α (°)		72.9800(19)
β (°)	113.588(2)	78.822(2)
γ (°)		84.6880(17)
Volume (Å^3)	1773.92(12)	550.46(3)
Z	4	1
D_{calcd} (Mg/m^3)	1.489	1.472
Absorption coefficient	1.416 mm^{-1}	1.171 mm^{-1}
Crystal size (mm^3)	0.38 x 0.34 x 0.20	0.45 x 0.34 x 0.30
θ range for data collection	2.85-27.49°	2.83-27.49°
Index range	-19 ≤ h ≤ 19	-9 ≤ h ≤ 9
	-9 ≤ k ≤ 10	-10 ≤ k ≤ 11
	-19 ≤ l ≤ 19	-12 ≤ l ≤ 12
Reflections collected	14312	7276
Independent reflections	4052	2495
	[R(int) = 0.0750]	[R(int) = 0.0644]
Goodness-of-fit on F^2	0.986	1.040
Final R indices [I>2σ(I)]	R1 = 0.0391	R1 = 0.0324
	wR2 = 0.0952	wR2 = 0.0811
R indices (all data)	R1 = 0.0750	R1 = 0.0359
	wR2 = 0.1128	wR2 = 0.0842

Results and Discussion

Descriptions of structures for 1 and 2

The structure of **1** consists of a 1D coordination polymer with a basic [Zn(**L1**)(maleate)] unit (Fig. 1.1). The maleate ligand in which two carboxylate groups are mutually arranged to *cis* through the carbon-carbon double bond bridges zinc(II) macrocycles. Two independent macrocycles are observed in the structure and each zinc atom sits on an inversion center. The macrocyclic ligand skeleton of **1** takes the most stable "trans III" conformation. The coordination environment about the central zinc(II) ion shows a distorted octahedron in the chain direction with four Zn-N and two Zn-O bonds. The Zn-N distances vary from 2.082(2) Å to 2.1150(19) Å with an average distance of ~ 2.102 Å, which are comparable to those found in related systems [8,9]. The Zn-O distances are in the range of 2.1968(16) Å - 2.2840(16) Å (Table 1.2). Those are well matched within the previously reported values ({Zn(**L**)(phthalate)}$_n$·(CH$_3$OH)$_{2n}$; Zn-O = 2.220(2), 2.190(2) Å [8], [Zn$_2$(Xylyl-bicyclam)(OAc)$_2$](OAc)$_2$·2CH$_3$OH; Zn-O = 2.089(2), 2.407(2) Å [6], {Zn(**L1**)(tp^{2-})·H$_2$O}$_n$; Zn-O = 2.1559(12) Å [9], {Zn(**L1**)(H$_2$bta^{2-})·2H$_2$O}$_n$;

Zn-O = 2.2839 (14) Å [9], Zn($L1$)(H$_2$btc$^-$)$_2$·2DMF; Zn-O = 2.2222(12) Å [9]; where tp = terephthalate, bta = 1,2,4,5-benzenetetracarboxylate and btc = 1,3,5-benzenetricarboxylate). The significant difference between the two Zn-O distances in **1** is ascribed to the different types of hydrogen bonding interactions involved. One of the pertinent structural features found in **1** is the pre-organization of N-H groups of the macrocycle with its role in profacial selection of maleate anion binding through covalent and hydrogen bonding interactions. Apart from the Zn-O bonds, the oxygen atoms O2 and O3 of the carboxylate groups participate in bifurcated hydrogen bonds (N1-H1…O2#1 = 2.861(3) Å, N4-H4…O2 = 2.914(3) Å, N3-H3…O3 = 3.014(3) Å, O1W-H1WA…O3 = 2.752(3) Å; symmetry code: #1 = -x+1, -y+1, -z+1) by connecting two macrocycles. It appears that the presence of such hydrogen bonding interactions is crucial for the formation of coordination polymer **1**. Water molecules mediate in connecting the macrocycles as well as in interconnecting each polymeric 1D chain through hydrogen bonding interactions (Table 1.3).
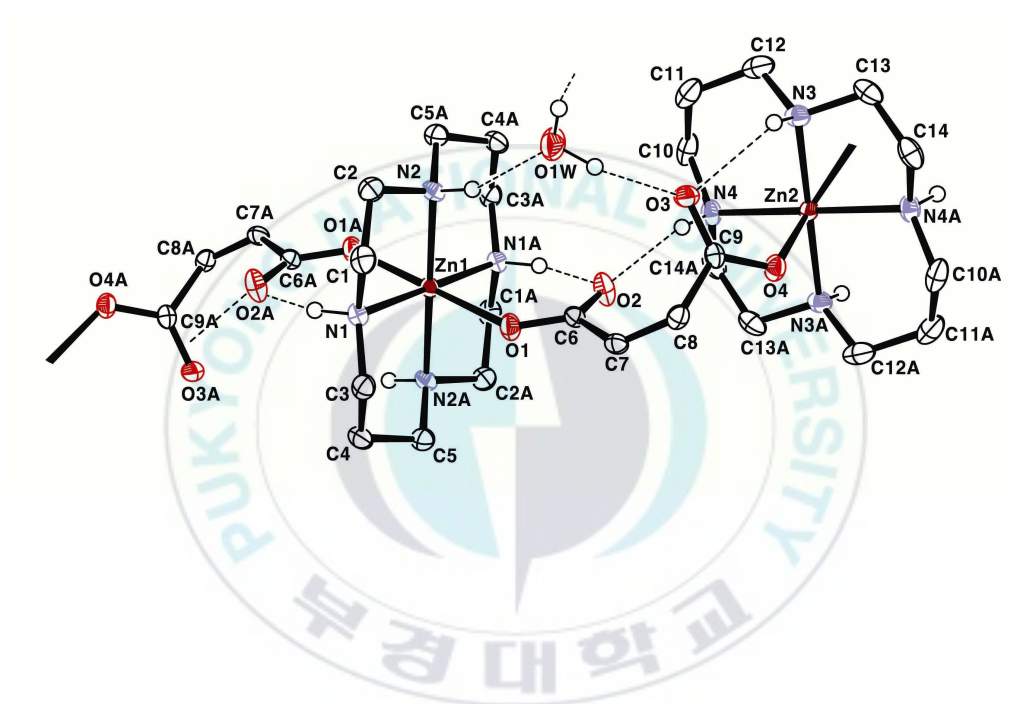
Figure 1.1. Molecular structure of {[Zn(**L1**)(maleate)]·H$_2$O}$_n$ (**1**) with atom-labeling scheme. Hydrogen atoms other than those participating in hydrogen bonding are omitted for clarity.

Table 1.2. Selected bond lengths (Å) and angles (°) for {[Zn(**L1**)(maleate)]·H_2O}$_n$ (**1**)

Zn1-N1	2.1018(19)
Zn1-N2	2.1150(19)
Zn2-N3	2.082(2)
Zn2-N4	2.1078(18)
Zn1-O1	2.1968(16)
Zn2-O4	2.2840(16)
N1-Zn1-N2	85.11(7)
N1-Zn1-O1	87.00(7)
N2-Zn1-O1	90.26(7)
N3-Zn2-N4	94.70(8)
N3-Zn2-O4	91.13(7)
N4-Zn2-O4	91.45(7)

Symmetry transformations used to generate equivalent atoms:

#1 -*x*+1,-*y*+1,-*z*+1   #2 -*x*+1,-*y*+1,-*z*

Table 1.3. Hydrogen bonds for {[Zn(**L1**)(maleate)]·H_2O}$_n$ (**1**) (Å and °)

D-H…A	d(D-H)	d(H…A)	d(D…A)	<(DHA)
N1-H1…O2#1	0.93	2.01	2.861(3)	151.8
N2-H2…O1W	0.93	2.06	2.947(3)	157.7
N3-H3…O3	0.93	2.28	3.014(3)	135.1
N4-H4…O2	0.93	2.06	2.914(3)	151.2
O1W-H1WB…O4#3	0.89(3)	2.16(3)	3.036(3)	169(3)
O1W-H1WA…O3	0.91(4)	1.86(4)	2.752(3)	168(3)

Symmetry transformations used to generate equivalent atoms:

#1 -*x*+1,-*y*+1,-*z*+1   #2 -*x*+1,-*y*+1,-*z*   #3 -*x*+3/2,*y*+1/2,-*z*+1/2

The structure of **2** consists of a mononuclear [Zn(**L1**)(H$_2$O)$_2$]$^{2+}$ divalent cation, a fumarate anion and solvent water molecules (Fig. 1.2). As the basicity of carboxylates in the fumarate anions is expected to be similar to that of maleate anions, it is surprising that the fumarate anions do not interact with zinc(II) cyclams. Instead, the water molecules preferentially coordinate to the zinc(II) ion in DMF/H$_2$O cosolvents. It appears that the presence of hydrogen bonding interactions in addition to the Zn-O covalent bond is requisite for the formation of coordination polymer. However, it is unfavorable for the fumarate anions in which two carboxylate groups are mutually *trans* to form such additional hydrogen bonds. The coordination geometry around the zinc(II) ion reveals a six coordinated axially distorted octahedron with four nitrogen atoms from the macrocycle and two oxygen atoms from water molecules. The Zn-N distances of 2.1063(15) Å – 2.0926(14) Å and the Zn-O distance of 2.2539(13) Å are normal and fall on those found in a closely related system ([Zn(**L1**)(H$_2$O)$_2$](OAc)$_2$; Zn-N = 2.1198(15) - 2.0809(15) Å, Zn-O = 2.2719(14) Å [8]) (Table 1.4).

In conclusion, we have prepared and fully characterized two new zinc(II) cyclams. The carboxylate groups of the maleate ligand in the complex **1** show strong coordination behavior toward the zinc(II) cyclam with hydrogen

bonding interactions between the N-H groups of the macrocycle and oxygen atoms of the maleate ligands. However, the fumarate anion having two *trans*-arranged carboxylate groups through the carbon-carbon double bond does not interact with the zinc(II) cyclam. From this account, we conclude that the coordination behavior of carboxylate groups of maleate or fumarate ligands to zinc(II) cyclams are highly dependent on the presence of additional hydrogen bonding interactions that reinforce the formation of coordination polymer. The zinc(II) complexes **1** and **2** could be good model systems for the understanding of the nature of molecular interactions between zinc(II) cyclams and carboxylate groups as well as the importance of the presence of hydrogen bonding interactions in forming coordination polymer.
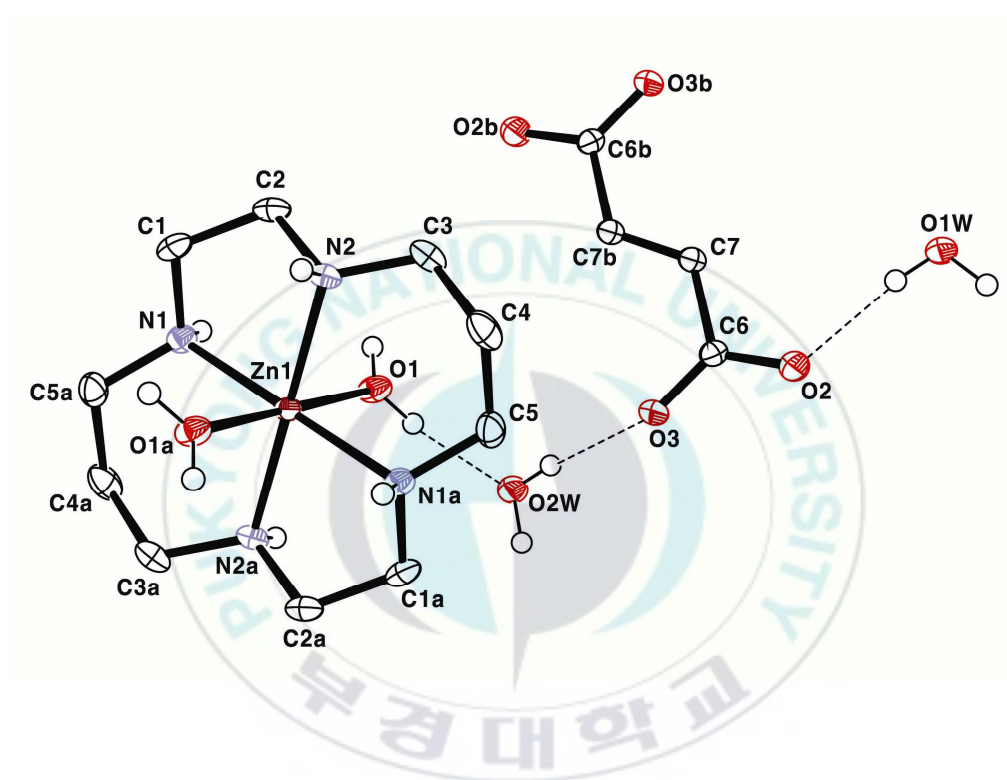
Figure 1.2. Molecular structure of [Zn(**L1**)(H$_2$O)$_2$](fumarate)·4H$_2$O (**2**) with atom-labeling scheme. Hydrogen atoms other than those participating in hydrogen bonding are omitted for clarity.

Table 1.4. Selected bond lengths (Å) and angles (^{o}) for [Zn(**L1**)(H$_2$O)$_2$](fumarate)·4H$_2$O (**2**)

Zn1-N1	2.1063(15)
Zn1-N2	2.0926(14)
Zn1-O1	2.2539(13)
N1-Zn1-N2	85.18(6)
N1-Zn1-O1	88.95(5)
N2-Zn1-O1	91.86(5)

Symmetry transformations used to generate equivalent atoms:

#1 -x+1,-y+1,-z+1   #2 -x,-y,-z+2

Table 1.5. Hydrogen bonds for (Å and °) [Zn(**L1**)(H$_2$O)$_2$](fumarate)·4H$_2$O (**2**)

D-H…A	d(D-H)	d(H…A)	d(D…A)	<(DHA)
N1-H1…O2W#3	0.93	2.21	3.074(2)	155.0
N2-H2…O1W#4	0.93	2.12	3.029(2)	166.4
O1-H2O…O2W	0.84(3)	1.98(3)	2.820(2)	172(3)
O1W-H1WB…O2	0.79(3)	1.93(3)	2.706(2)	173(3)
O1W-H1WA…O2#5	0.82(3)	1.91(3)	2.7066(19)	163(3)
O2W-H2WB…O3	0.76(3)	2.06(3)	2.813(2)	170(3)
O1-H1O…O1W#2	0.83(3)	1.90(3)	2.7133(19)	168(3)
O2W-H2WA…O3#6	0.85(3)	1.93(3)	2.7758(19)	174(3)

Symmetry transformations used to generate equivalent atoms:

#1 -x+1,-y+1,-z+1   #2 -x,-y,-z+2   #3 -x,-y+1,-z+1

#4 -x+1,-y,-z+2   #5 -x,-y,-z+3   #6 -x,-y+1,-z+2

*Spectroscopic properties and thermal analysis for **1** and **2***

The solid state infrared spectrum of **1** indicates a νO-H band at 3349cm^{-1}, νN-H band at 3209cm^{-1}and νCOO$^-$ bands at 1569, 1300cm^{-1}, supporting the crystal structure clearly (Fig. 1.3 (a)). The spectrum of **2** contains a νO-H band at 3379cm^{-1}, νN-H band at 3174cm^{-1}and νCOO$^-$ bands at 1694, 1554cm^{-1} (Fig. 1.3 (b)). TGA-DTG curves for **1** showed a first weight loss of 4.5 % (calculated 4.5%) over 85 - 140 ^{o}C with an endothermic processes centered at 126 ^{o}C, corresponding to the loss of a molecule of water. On further heating, gradual weight loss was observed in 275 - 585 ^{o}C range with the loss of maleate and cyclam ligands. Finally, the ZnO residue (observed 20.4 %, calculated 20.4 %) was remained above 585 ^{o}C (Fig. 1.4 (a)). For complex **2**, the TGA analysis was hampered by its thermal unstability even at room temperature. It was only possible to identify the dehydration of six water molecules (two coordinated and four uncoordinated), which started even at ~ 26 ^{o}C and completed with the weight loss of 23.5% (calculated 22.1%) at 105 ^{o}C. Significant weight loss was observed gradually on further heating presumably due to the loss of the macrocyclic ligand and the fumarate anion. No residues were observed above 950 ^{o}C (Fig. 1.4 (b)).
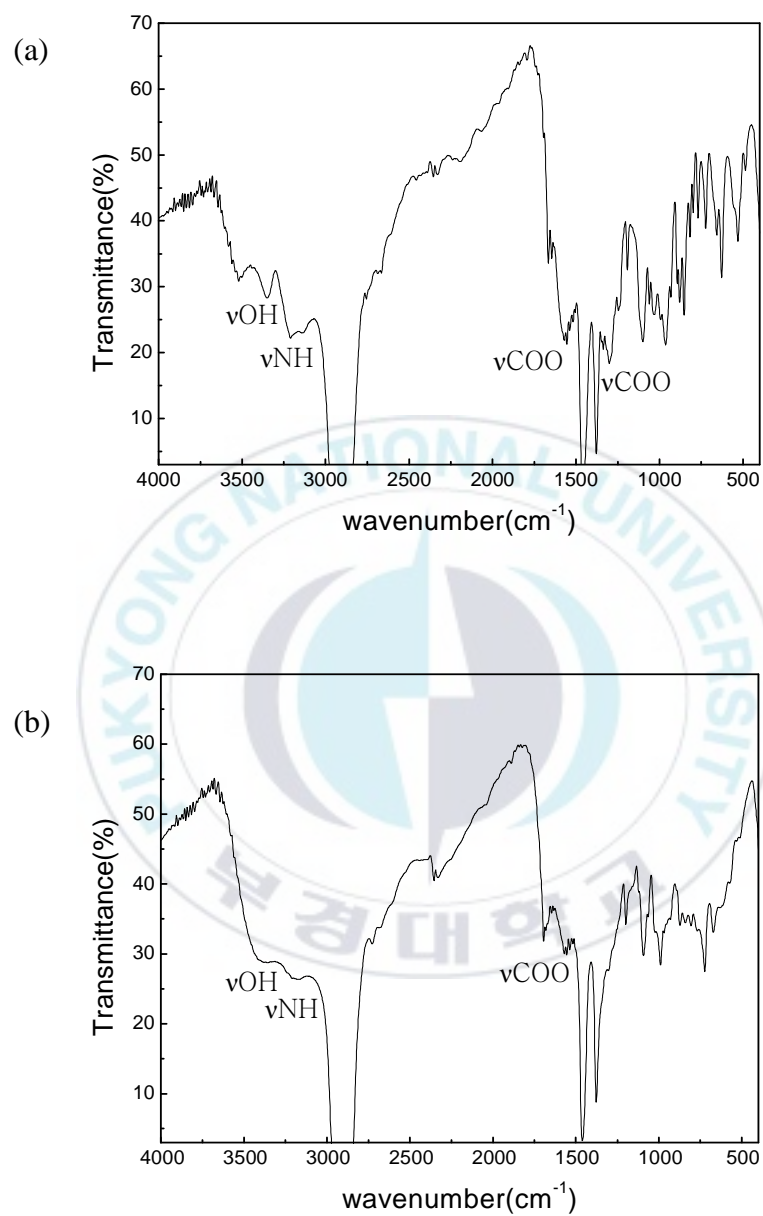
Figure 1.3. Infrared spectra of (a) $\{[Zn(\textbf{L1})(\text{maleate})]\cdot H_2O\}_n$ (**1**) and (b) $[Zn(\textbf{L1})(H_2O)_2](\text{fumarate})\cdot 4H_2O$ (**2**) [Nujol mull]
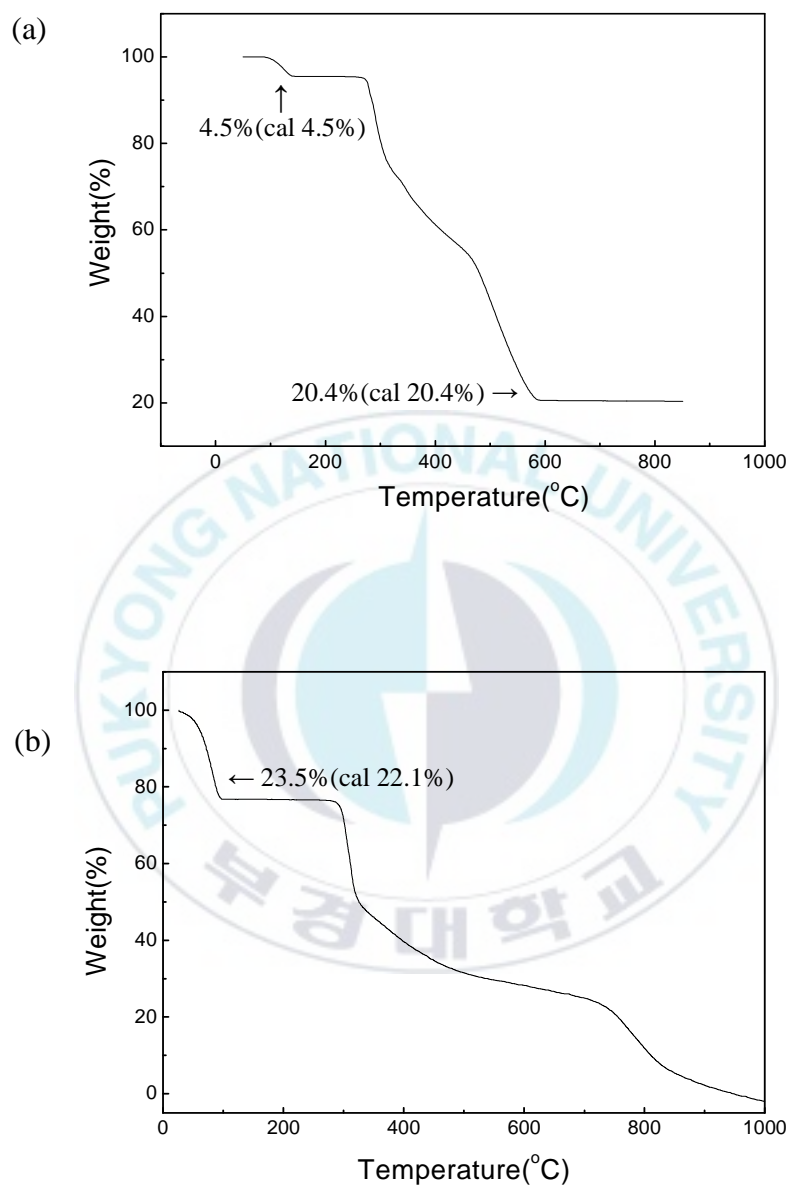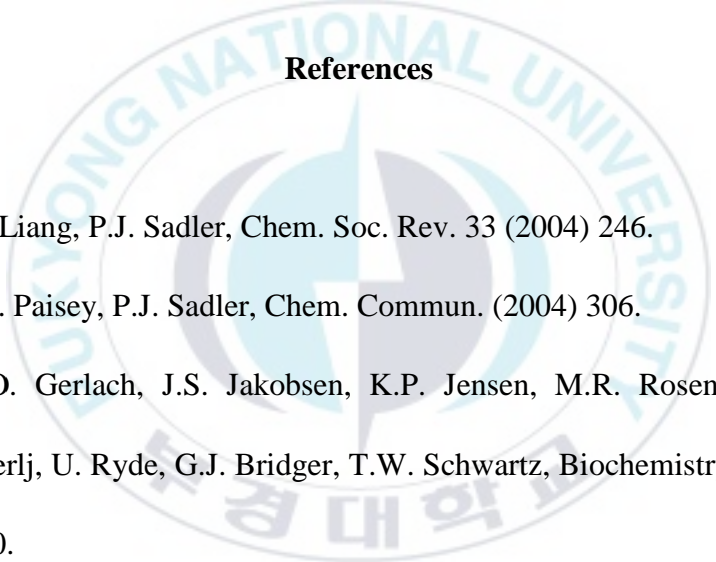
Figure 1.4. Thermogravimetric analyses of (a) $\{[Zn(\mathbf{L1})(maleate)]\cdot H_2O\}_n$ (**1**) and (b) $[Zn(\mathbf{L1})(H_2O)_2](fumarate)\cdot 4H_2O$ (**2**)

Supplementary material

Crystallographic data have been deposited at the Cambridge Crystallographic Data Center (CCDC), CCDC Nos. 295277 for **1** and 295278 for **2**.

References

[1]   X. Liang, P.J. Sadler, Chem. Soc. Rev. 33 (2004) 246.

[2]   S.J. Paisey, P.J. Sadler, Chem. Commun. (2004) 306.

[3]   L.O. Gerlach, J.S. Jakobsen, K.P. Jensen, M.R. Rosenkilde, R.T. Skerlj, U. Ryde, G.J. Bridger, T.W. Schwartz, Biochemistry 42 (2003) 710.

[4]   E. De Clercq, N. Yamamoto, R. Pauwels, J. Balzarini, M. Witvrouw, K. De Vreese, Z. Debyser, B. Rosenwirth, P. Peichl, R. Datema, Antimicrob. Agents Chemother. 38 (1994) 668.

[5]   E. De clercq, N. Yamamoto, R. Pauwels, M. Baba, D. Schols, H. Nakashima, J. Balzarini, Z. Debyser, B.A. Murrer, D. Schwartz, D. Thornton, G. Bridger, S. Fricker, G. Henson, M. Abrams, D. Picker,

Proc. Natl. Acad. Sci. USA 89 (1992) 5286.

[6] X. Liang, J.A. Parkinson, M. Weishäupl, R.O. Gould, S.J. Paisey, H. Park, T.M. Hunter, C.A. Blindauer, S. Parsons, P.J. Sadler, J. Am. Chem. Soc. 124 (2002) 9105.

[7] L.O. Gerlach, R.T. Skerlj, G.J. Bridger, T.W. Schwartz, J. Biol. Chem. 276 (2001) 14153.

[8] X. Liang, M. Weishäupl, J. A. Parkinson, S. Parsons, P.A. McGregor, P.J. Sadler, Chem. Eur. J. 9 (2003) 4709.

[9] H. Jo, A.J. Lough, J.C. Kim, Inorg. Chim. Acta, 358 (2005) 1274.

[10] Z. Otwinowski, W. Minor, Meth. Enzymol. 276 (1997) 1783.

[11] G.M. Sheldrick, SHELXTL\PC V5.1, Bruker Analytical X-ray Systems, Madison, WI, 1997.

CHAPTER II

Different coordination modes of Hdipic and dipic ligands to nickel(II) ions in a same environment

Abstract

Two new nickel(II) complexes of the composition $[Ni(L1)(Hdipic)_2] \cdot 2H_2O$ (**1**) and $[Ni(L1)(H_2O)_2][Ni(dipic)_2] \cdot 2.5H_2O$ (**2**) (**L1** = 1,4,8,11-tetraazacyclotetradecane, cyclam, dipic = 2,6-pyridinedicarboxylate, dipicolinate) have been prepared and structurally characterized by a combination of analytical, spectroscopic, thermogravimetric, and crystallographic methods. The structure of **1** shows that the central nickel(II) ion is coordinated axially by two monodentate Hdipic ligands. The discrete neutral complex **1** further extends its structure by hydrogen bonding interactions to form a one-dimensional supramolecule. The mononuclear motif $[Ni(L1)(Hdipic)_2]$ acts not only as hydrogen bond acceptors but also as hydrogen bond donors, thus, it behaves as a "metal complex synthon". In addition, the π - π interaction is observed between the Hdipic ligands. The

structure of **2** consists of two independent nickel(II) centers. Water molecules instead of dipic ligands prefer to coordinate to the Ni1 ion forming a divalent cation $[Ni(\mathbf{L1})(H_2O)_2]^{2+}$. Two dipic ligands coordinate to the second Ni2 ion forming a divalent anion $[Ni(dipic)_2]^{2-}$. The divalent cations and anions are charge-balanced, resulting in a molecular salt. The divalent cations and anions are interconnected by multiple types of hydrogen bonding interactions.

Introduction

Research on transition metal complexes with polycarboxylates has been the subject of numerous reports [1-4]. The reasons for this interest mainly lie in their relevance to the development of more effective anti-HIV agents [2,5,6], the design of insulin-mimetic agents [7,8] and other potential applications [9,10]. Dipicolinate is one of the frequently used aromatic polycarboxylates in those areas. The interest of metal complexes with dipic and its protonated forms Hdipic and H_2dipic stems from their interesting structural features with various coordination modes [7], stabilization of unusual oxidation states [11], chemical analysis of iron at low concentration [12], insulin-mimetic effects [7,8], and catalysis [13]. As part of our study on understanding the interactions

between macrocyclic transition metal complexes and aromatic ploycarboxylates, we were interested in preparing and characterizing nickel(II) complexes containing dipicolinate ligands. Herein, we report the synthesis, crystal structures and properties of **1** and **2**.
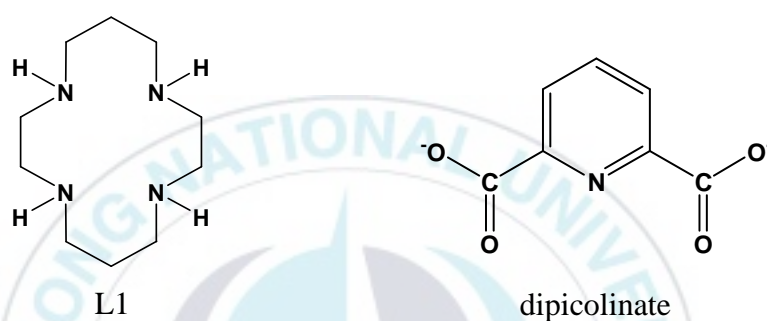
L1   dipicolinate

Experimental

Materials and Methods

All chemicals used in the synthesis were reagent grade and used without further purification. Distilled water was used for all procedures. Infrared spectra of solid samples were recorded on a Perkin-Elmer Paragon 1000 FT-IR spectrophotometer between $4000 cm^{-1}$ and $400 cm^{-1}$ as Nujol mulls on KBr discs. Thermal analysis (TGA-DTG) was performed on a Perkin-Elmer Model

TGA-7 Thermogravimetric Analyzer under air from 50 to 800 ^{o}C at a heating rate of 10 ^{o}C/min. Elemental analysis was performed by the Korea Research Institute of Chemical Technology, Daejeon, Korea. Solid state diffuse reflectance spectra were obtained at the Kanazawa University, Japan. [Ni(**L1**)][ClO$_4$]$_2$ [14] and [Ni(**L1**)][PF$_6$]$_2$ [15] were prepared as described in the literature.

*Synthesis of **1** and **2***

To a DMF solution of [Ni(**L1**)][PF$_6$]$_2$ (274 mg, 0.5 mmol) was added a DMF solution of H$_2$dipic (167 mg, 1.0 mmol). The mixture was allowed in an open beaker at room temperature. Purple blocks of **1** and green needles of **2** were obtained simultaneously in a week. Suitable crystals of **1** and **2** for X-ray diffraction studies and other measurements were manually collected under the microscope. Anal. Calcd. for C$_{24}$H$_{36}$N$_6$O$_{10}$Ni (**1**) (Yield > 90%): C, 45.91; H, 5.74; N, 13.39%. Found: C, 45.93; H, 5.69; N, 13.31%. Anal. Calcd. for C$_{24}$H$_{39}$N$_6$O$_{12.5}$Ni$_2$ (**2**) (Yield < 10%): C, 39.50; H, 5.35; N, 11.52%. Found: C, 39.51; H, 5.29; N, 11.50 %.

X-ray crystallography

X-ray crystallographic data for **1** and **2** were collected on a Nonius Kappa CCD diffractometer, using graphite monochromated Mo K_α radiation (λ = 0.71073 Å). A combination of 1º ϕ and ω (with κ offsets) scans were used to collect sufficient data. The data frames were integrated and scaled using the Denzo-SMN package [16]. The structure was solved and refined using the SHELXTL\PC V5.1 package [17]. Refinement was performed by full-matrix least squares on F^2 using all data (negative intensities included). Hydrogen atoms were included in calculated positions, except for those involving in hydrogen bonding specifically for the hydrogen atoms bonded to the nitrogen atoms, which were refined with isotropic thermal parameters. The data collection and refinement details are presented in Table 2.1.

Table 2.1. Crystal data and structure refinement for [Ni(**L1**)(Hdipic)$_2$]·2H$_2$O (**1**) and [Ni(**L1**)(H$_2$O)$_2$][Ni(dipic)$_2$]·2.5H$_2$O (**2**)

	1	2
Empirical formula	C$_{24}$H$_{36}$N$_6$O$_{10}$Ni	C$_{24}$H$_{39}$N$_6$O$_{12.5}$Ni$_2$
Formula weight	627.30	729.03
Temperature (K)	150(1)	150(1)
Crystal system	Triclinic	Monoclinic
Space group	P -1	C2/c
a (Å)	8.0569(3)	22.6811(9)
b (Å)	8.2784(5)	15.1030(7)
c (Å)	11.5014(8)	8.8806(2)
α (°)	74.463(3)	
β (°)	85.675(4)	102.066(2)
γ (°)	67.097(3)	
Volume (Å^3)	680.47(7)	2974.87(19)
Z	1	4
D$_{calcd}$ (Mg/m^3)	1.531	1.628
Absorption coefficient	0.781 mm^{-1}	1.340 mm^{-1}
Crystal size (mm^3)	0.18 x 0.10 x 0.08	0.30 x 0.20 x 0.14
θ range for data collection	2.77-27.54°	2.69-27.49°
Index range	-10 ≤ h ≤ 10	-29 ≤ h ≤ 28
	-9 ≤ k ≤ 10	-17 ≤ k ≤ 19
	-14 ≤ l ≤ 14	-10 ≤ l ≤ 11
Reflections collected	6133	10596
Independent reflections	3055	3404
	[R(int) = 0.0614]	[R(int) = 0.0480]
Goodness-of-fit on F^2	1.042	1.060
Final R indices [I>2σ(I)]	R1 = 0.0453	R1 = 0.0371
	wR2 = 0.0973	wR2 = 0.0824
R indices (all data)	R1 = 0.0728	R1 = 0.0594
	wR2 = 0.1233	wR2 = 0.0923

Results and discussion

Descriptions of structures for 1 and 2

Treatment of [Ni(**L1**)][PF$_6$]$_2$ with two equivalents of H$_2$dipic in DMF provided purple blocks of **1** and green needles of **2** on slow evaporation. Compounds **1** and **2** were stable indefinitely in air, and the microanalytical and infrared spectral results clearly supported the structures determined by X-ray diffraction studies.

The structure of **1** shows that the central nickel(II) ion is coordinated axially by two Hdipic ligands (Fig. 2.1). The macrocyclic ligand skeleton in **1** takes the most stable "*trans* III" conformation as usual. The coordination environment around the central nickel(II) ion can be described as a distorted octahedron with four Ni-N and two Ni-O bonds. The Ni atom sits on an inversion center. The Ni-N distances vary from 2.067(2) Å to 2.073(2) Å, which are typical for a six-coordinated nickel(II) d^8 system [1,18]. The Ni-O distance of 2.1242(19) Å lies within the previously reported values ({[Ni(**L**)(dipic)$_2$]·H$_2$O}$_n$ (**L** = 2,5,9,12-tetramethyl-1,4,8,11-tetraazacyclotetradecane) [18]; Ni-O = 2.115(4), 2.086(4) Å,

[Ni$_2$(dipic)$_2$(H$_2$O)$_5$]·2H$_2$O [19]; Ni-O = 2.098(3), 2.159(3), 2.164(3), 2.179(3) Å). Although dipicolinates have a unique ability to form stable chelates, the Hdipic ligand in **1** acts as a monodentate ligand by coordination of one oxygen atom from each carboxylate group to the nickel(II) ion. It is known that there is a range of different coordination modes with possible monodentate [20], bidentate [8,21], tridentate [7,8,20,23,24], or bridging [18,19,22] in transition metal-dipicolinate complexes depending on whether the divalent anionic dipic, protonated anionic Hdipic or diprotonated H$_2$dipic forms are coordinated to metal ions (Fig. 2.2). The discrete neutral complex **1** further extends its structure by hydrogen bonding interactions to form a one-dimensional supramolecule {[Ni(**L1**)(Hdipic)$_2$]·2H$_2$O}$_n$ (Fig. 2.3 and Table 2.3). The mononuclear motif [Ni(**L1**)(Hdipic)$_2$] acts not only as hydrogen bond donors but also as hydrogen bond acceptors, thus, it behaves as a "metal complex synthon". In addition, the π - π interactions are observed between the Hdipic ligands (Fig. 2.3). In a closely related system reported recently [18], a one-dimensional coordination polymer {[Ni(**L**)(dipic)$_2$]·2H$_2$O}$_n$ has been built by the reaction between [Ni(**L**)(H$_2$O)$_2$][Cl]$_2$ and dipic, where the macrocyclic units are bridged by a dipic anion with a bis-monodentate coordination mode.
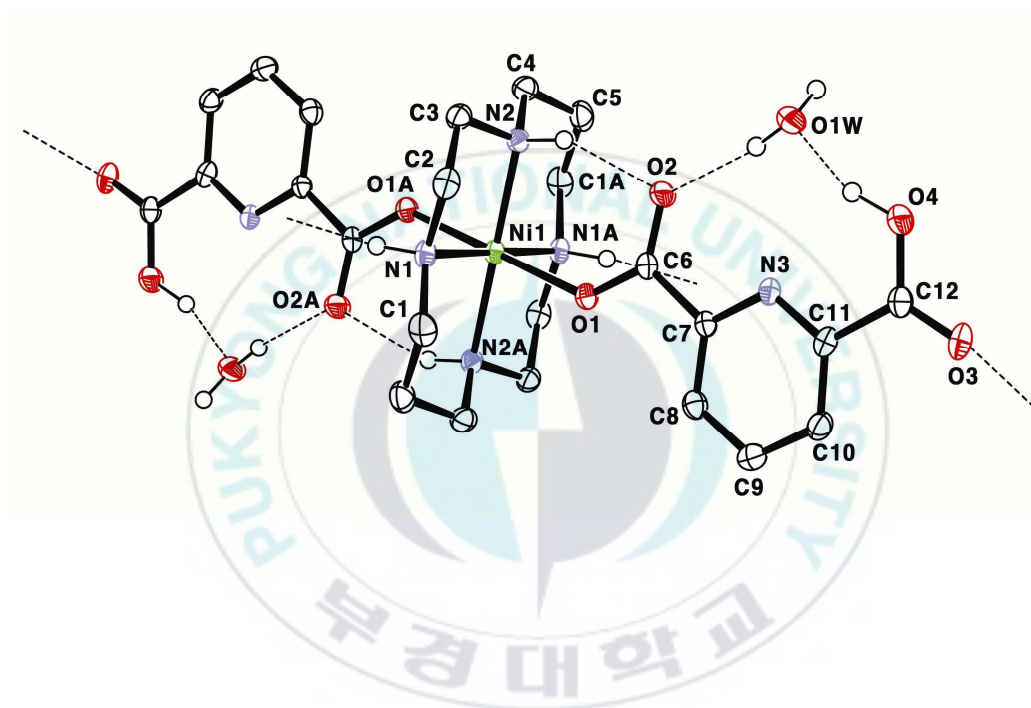
Figure 2.1. Molecular structure of [Ni(**L1**)(Hdipic)$_2$]·2H$_2$O (**1**) with atom-labeling scheme. Hydrogen atoms other than those participating in hydrogen bonding are omitted for clarity.

Table 2.2. Selected bond lengths (Å) and angles (°) for [Ni(**L1**)(Hdipic)$_2$]·2H$_2$O (**1**)

Ni1-N1	2.067(2)
Ni1-N2	2.073(2)
Ni1-O1	2.1242(19)
C6-O1	1.265(3)
C6-O2	1.251(3)
C12-O3	1.213(3)
C12-O4	1.328(4)
N1-Ni1-N2#1	94.73(9)
N1-Ni1-N2	85.27(9)
N1-Ni1-O1#1	89.57(9)
N1-Ni1-O1	90.43(9)
N2-Ni1-O1	92.49(8)

Symmetry transformations used to generate equivalent atoms:

#1 -*x*+1,-*y*+1,-*z*+1

Table 2.3. Hydrogen bonds for [Ni(**L1**)(Hdipic)$_2$]·2H$_2$O (**1**) (Å and °)

D-H…A	d(D-H)	d(H…A)	d(D…A)	<(DHA)
N1-H1…O3#2	0.93	2.12	2.955(3)	149.5
N2-H2…O2	0.93	2.06	2.916(3)	151.7
O1W-H1WA…O4#3	0.90(5)	2.13(5)	2.961(3)	154(4)
O1W-H2WA…O2	0.82(5)	1.97(5)	2.787(3)	171(4)
O4-H4O…O1W	0.99(5)	1.68(5)	2.634(3)	161(5)

Symmetry transformations used to generate equivalent atoms:

#1 -*x*+1,-*y*+1,-*z*+1   #2 *x*,*y*+1,*z*-1   #3 -*x*,-*y*,-*z*+2
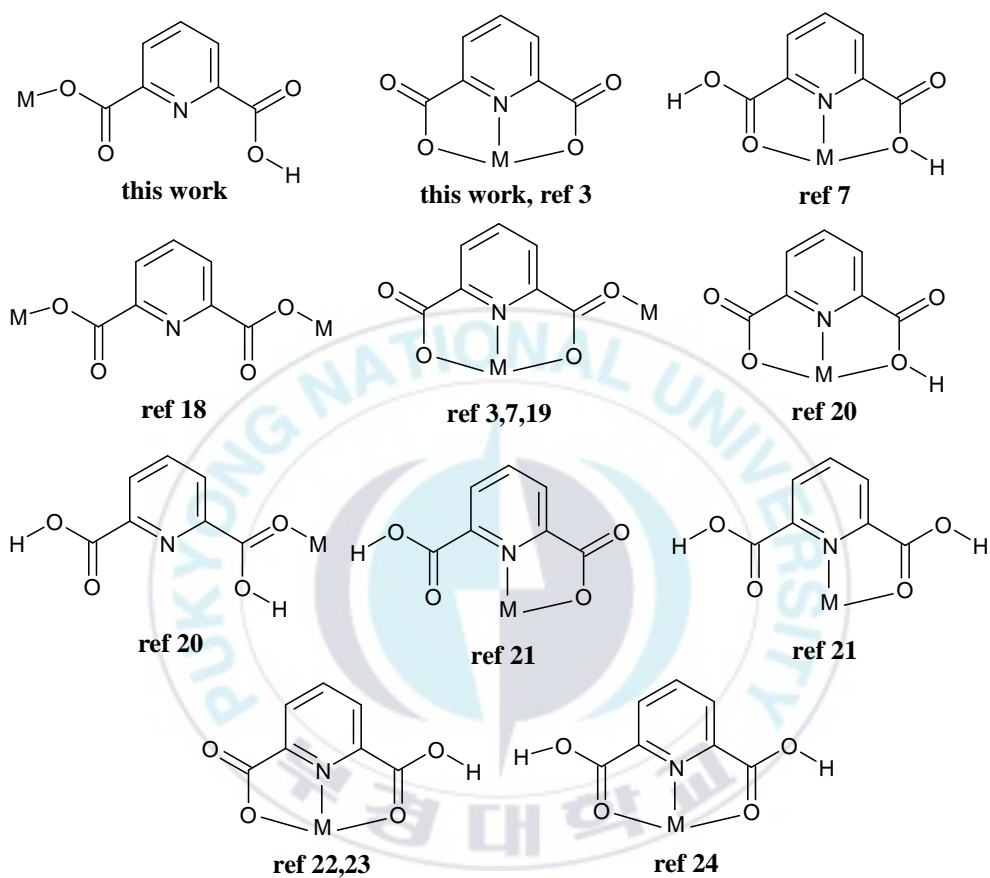
Figure 2.2. Versatility of coordination modes for metal-H_2dipic, Hdipic and dipic.
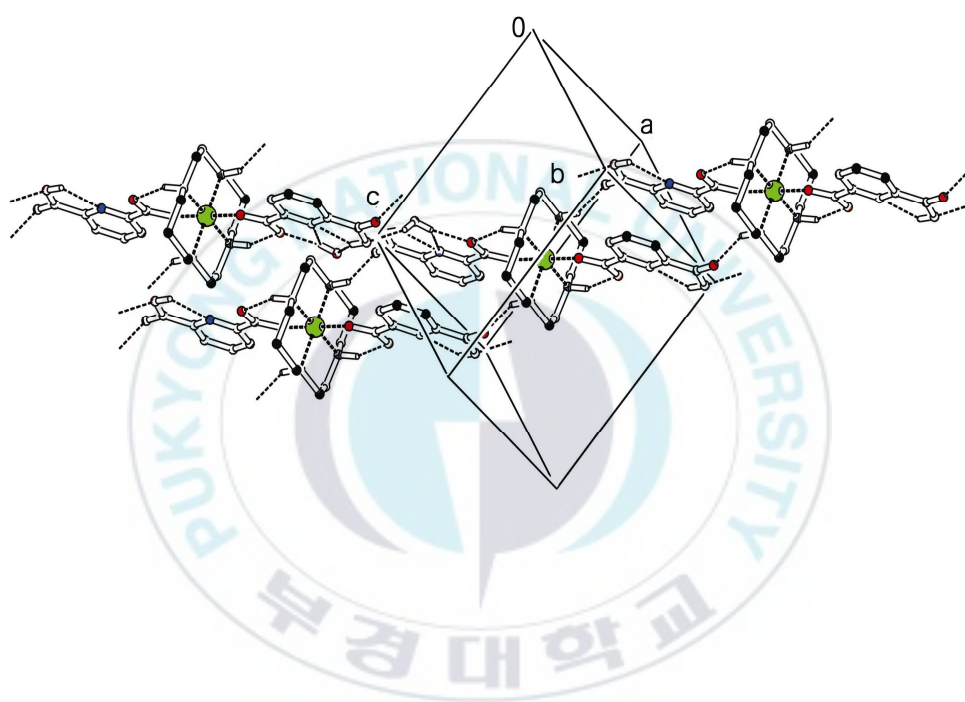
Figure 2.3. View of 1D supramolecule structure of

{[Ni(**L1**)(Hdipic)$_2$]·2H$_2$O}$_n$ (**1**). Dotted lines indicated hydrogen bonds.

The green complex **2** was obtained simultaneously during the preparation of

1 as a minor product. As shown in Fig. 2.4, The water ligands instead of dipic

anions preferentially coordinate to the atom Ni1, forming a $[Ni(\mathbf{L1})(H_2O)_2]^{2+}$

divalent cation. The atom Ni2 is coordinated by two dipic ligands *via* their

carboxylate and nitrogen donors resulting in the formation of a $[Ni(dipic)_2]^{2-}$

divalent anion. Eventually, the $[Ni(dipic)_2]^{2-}$ divalent anion is charge-balanced

by the $[Ni(\mathbf{L1})(H_2O)_2]^{2+}$ divalent cation. Since the purity of starting material

$[Ni(\mathbf{L1})][PF_6]_2$ is high enough by repeated recrystallization, the Ni2 ion in the

divalent anion seems to be originated from the $[Ni(\mathbf{L1})]^{2+}$ divalent cation. The

planes defining the dipic rings are mutually orthogonal in the $[Ni(dipic)_2]^{2-}$.

Both of the nickel(II) ions exhibit distorted octahedral geometry. The Ni1-N

bond distances are 2.062(2) and 2.0733(19) Å, and the Ni1-O bond distance is

2.1524(18) Å. The Ni2-N_d (d = dipic) bond distances are 1.931(3) and

1.955(3) Å, and the Ni2-O bond distances are 2.1464(16) and 2.1318(17) Å

(Table 2.4). Those are comparable with values in systems

$([Ni(\mathbf{L1})(H_2O)_2]_3[C_6H_3(COO)_3]_2·24H_2O$ [1]; Ni-N = 2.070(3), 2.057(3) Å,

$\{[Ni(\mathbf{L})(dipic)_2]·H_2O\}_n$ [18]; Ni-N = 2.070(4), 2.087(5), 2.084(5), 2.090(5) Å,

Ni-O = 2.115(4), 2.086(4) Å, $[Ni_2(dipic)_2(H_2O)_5]·2H_2O$; Ni-O = 2.098(3),

2.159(3), 2.164(3), 2.179(3) Å, Ni-N_d = 1.962(3), 1.974(3) Å) [19]. The

carboxylate groups of dipic ligands are bound to Ni2 in a most frequently observed *O,N,O'*-tridentate coordination mode (Fig. 2.4). The independent divalent cations and anions are interconnected by multiple types of hydrogen bonding interactions (Table 2.5).

In conclusion, we have prepared and fully characterized two new carboxylato nickel(II) complex **1** and **2**. The Hdipic ligands in **1** act as a monodentate ligand by coordination of one oxygen atom from each carboxylate group to the nickel(II) ion. The resulting neutral motif [Ni(**L1**)(Hdipic)$_2$]·2H$_2$O extends its structure to form the supramolecule by intermolecular hydrogen bonds and π - π interactions. In the complex **2**, water molecules instead of dipic ligands prefer to coordinate to the Ni1 ion, forming the divalent cation [Ni(**L1**)(H$_2$O)$_2$]$^{2+}$. Two dipic ligands coordinate to the second Ni2 ion in a *O,N,O'*-tridentate coordination mode, forming the divalent anion [Ni(dipic)$_2$]$^{2-}$. The divalent cations and anions are charge-balanced, resulting in a molecular salt. The divalent cations and anions are interconnected by multiple types of hydrogen bonding interactions. The degree of deprotonation of H$_2$dipic is an important factor for the formation of complexes **1** and **2** even in a same reaction environment.
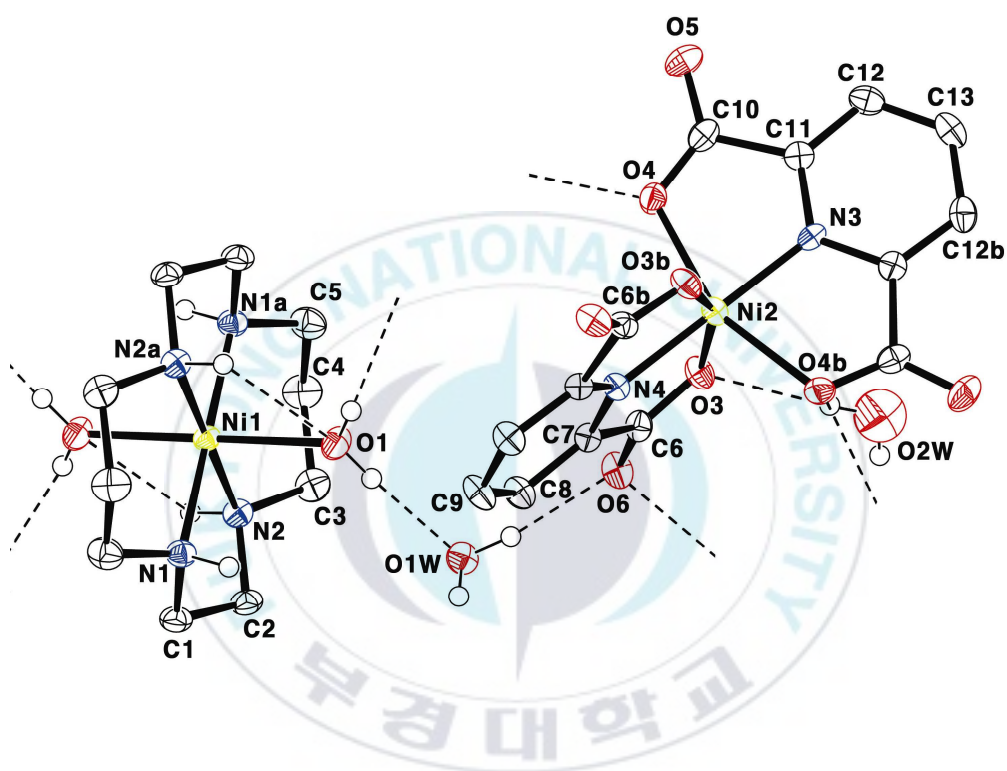
Figure 2.4. Molecular structure of [Ni(**L1**)(H$_2$O)$_2$][Ni(dipic)$_2$]·2.5H$_2$O (**2**) with atom-labeling scheme. Hydrogen atoms other than those participating in hydrogen bonding are omitted for clarity.

Table 2.4. Selected bond lengths (Å) and angles (^{o}) for
[Ni(**L1**)(H$_2$O)$_2$][Ni(dipic)$_2$]·2.5H$_2$O (**2**)

Ni1-N1	2.062(2)
Ni1-N2	2.0733(19)
Ni1-O1	2.1524(18)
Ni2-N3	1.931(3)
Ni2-N4	1.955(3)
Ni2-O4	2.1318(17)
Ni2-O3	2.1464(16)
C10-O4	1.272(3)
C10-O5	1.236(3)
N1-Ni1-N2#1	94.46(8)
N1-Ni1-N2	85.54(8)
N1#1-Ni1-O1	90.67(8)
N1-Ni1-O1	89.33(8)
N2-Ni1-O1	92.64(8)
N2-Ni1-O1#1	87.36(8)
N3-Ni2-O4	78.35(5)
N4-Ni2-O4	101.65(5)
O4-Ni2-O4#2	156.70(10)
O4-Ni2-O3#2	94.07(6)
N3-Ni2-O3	101.71(5)
N4-Ni2-O3	78.29(5)
O4-Ni2-O3	90.63(6)
O3#2-Ni2-O3	156.59(9)

Symmetry transformations used to generate equivalent atoms:

#1 -x+1/2,-y+3/2,-z #2 –x+1,y,-z+1/2

Table 2.5. Hydrogen bonds for [Ni(**L1**)(H$_2$O)$_2$][Ni(dipic)$_2$]·2.5H$_2$O (**2**) (Å and °)

D-H…A	d(D-H)	d(H…A)	d(D…A)	<(DHA)
O1-H1OA…O1W	0.80(4)	1.97(4)	2.771(3)	177(4)
O1-H1OB…O6#3	0.78(4)	2.02(4)	2.794(3)	171(3)
N1-H1…O5#4	0.93	2.21	2.975(3)	139.5
N2-H2…O3#5	0.93	2.30	3.176(3)	157.7
O1W-H1WA…O6	0.83(3)	1.99(3)	2.815(3)	171(3)
O1W-H1WB…O4#4	0.83(3)	2.00(4)	2.822(3)	176(3)
O2W-H2WA…O3	0.8400(12)	2.143(19)	2.981(12)	175(18)
O2W-H2WB…O5#6	0.8400(10)	2.24(11)	2.898(12)	136(14)

Symmetry transformations used to generate equivalent atoms:

#1 -x+1/2,-y+3/2,-z #2 -x+1,y,-z+1/2   #3 x,-y+1,z-1/2

#4 x,-y+1,z-1/2   #5 -x+1/2,y+1/2,-z+1/2   #6 x,y,z+1

*Spectroscopic properties, electronic spectra and thermal analysis of **1** and **2***

The solid state infrared spectrum of **1** indicates a νO-H band at 3579cm^{-1}, νN-H bands at 3283, 3172cm^{-1}, ν_{as} COO band from COOH at 1736cm^{-1}, ν_{as} COO bands from COO$^-$ at 1606, 1569cm^{-1} and ν_s COO bands from COO$^-$ at 1429, 1335cm^{-1}, supporting the crystal structure clearly (Fig. 2.5 (a)). The spectrum of **2** contains a νO-H band at 3350cm^{-1}, νN-H band at 3239cm^{-1}, ν_{as} COO band from COO$^-$ at 1607cm^{-1} and ν_s COO band from COO$^-$ at 1431cm^{-1} (Fig. 2.5 (b)).

Solid state diffuse reflectance spectra of **1** and **2** showed bands at 513, 690 nm for **1** and 525, 634 nm for **2** (Fig. 2.6). These are the characteristic spectra expected for a high-spin d^8 nickel(II) ions in a distorted octahedral environment, and could be attributed to $^3B_{1g}$ $^3E_g{}^b$, $^3B_{1g}$ $^3B_{2g} + {}^3B_{1g}$ $^3A_{2g}{}^a$ transitions, respectively. The expected highest energy bands at ca. 300 nm originated from $^3B_{1g}$ $^3E_g{}^c$ transitions were not resolved due to the strong charge transfer bands in both complexes [25,26].

TGA-DTG curves for **1** showed a first weight loss of 5.8 % (calculated 5.7 %) over 150 - 210 ^{o}C with an endothermic processes centered at 193 ^{o}C, corresponding to the loss of two water molecules. On further heating, gradual

weight loss was observed in 210 - 440 ^{o}C range with the loss of the macrocycle and Hdipic ligands. Finally, the NiO residue (observed 11.5 %, calculated 11.9 %) was remained above 440 ^{o}C. The TGA-DTG curves for **2** showed a first weight loss of 11.4 % (calculated 11.1 %) over 68 - 120 ^{o}C with an endothermic processes centered at 100 ^{o}C, corresponding to the loss of coordinated and lattice water molecules. On further heating, abrupt weight loss was observed in 330 - 411 ^{o}C range with the loss of the macrocycle and dipic ligands. Final residue (observed 18.5 %, calculated 18.3 %) was remained above 411 ^{o}C with Ni_2O composition (Fig. 2.7).
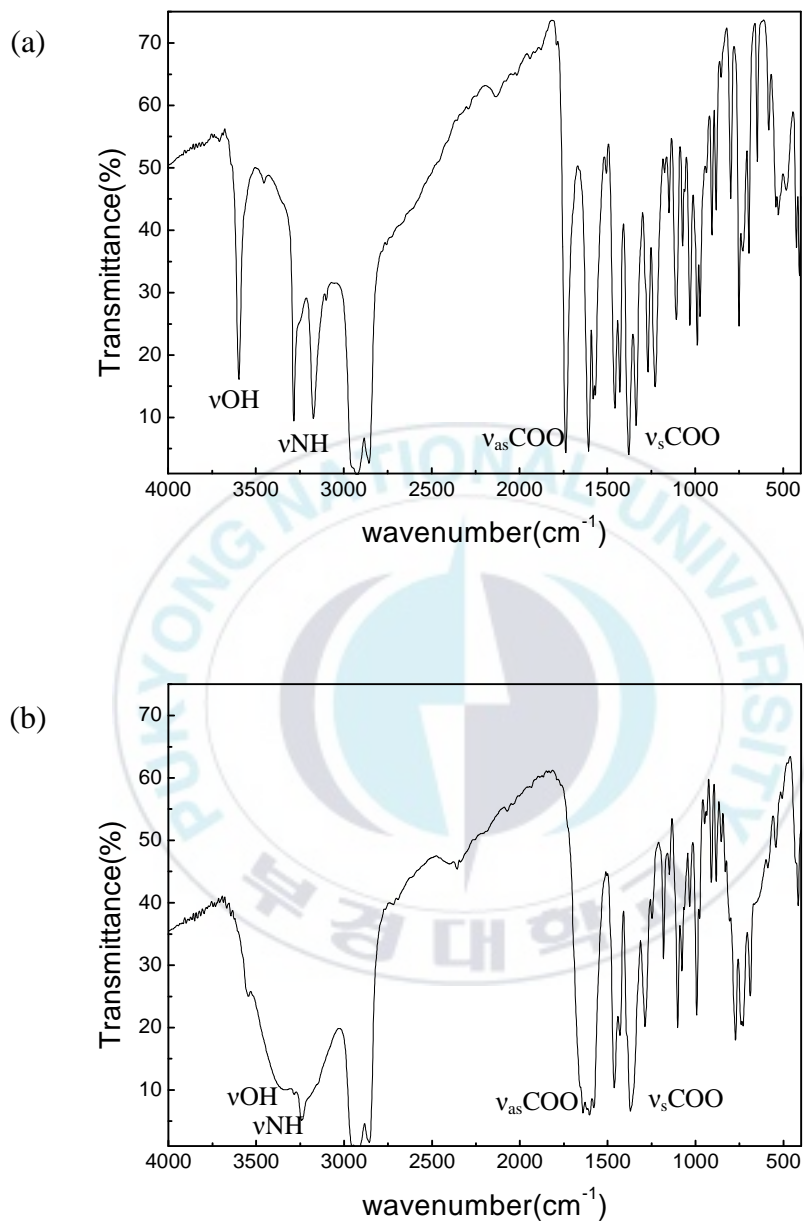
Figure 2.5. Infrared spectra of (a) [Ni(**L1**)(Hdipic)$_2$]·2H$_2$O (**1**) and (b) [Ni(**L1**)(H$_2$O)$_2$][Ni(dipic)$_2$]·2.5H$_2$O (**2**) [Nujol mull]
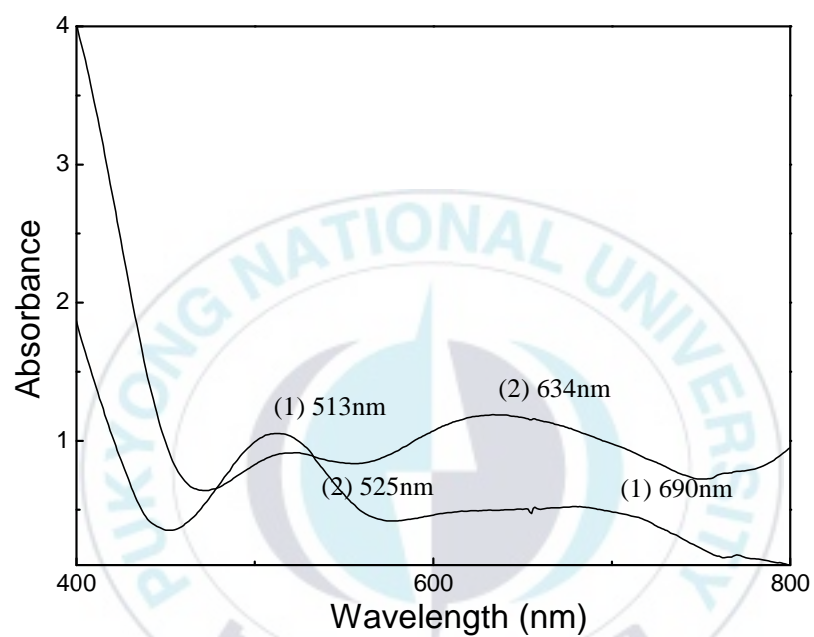
Figure 2.6. Solid state electronic absorption spectra of **1** and **2** by diffuse reflectance method at room temperature.
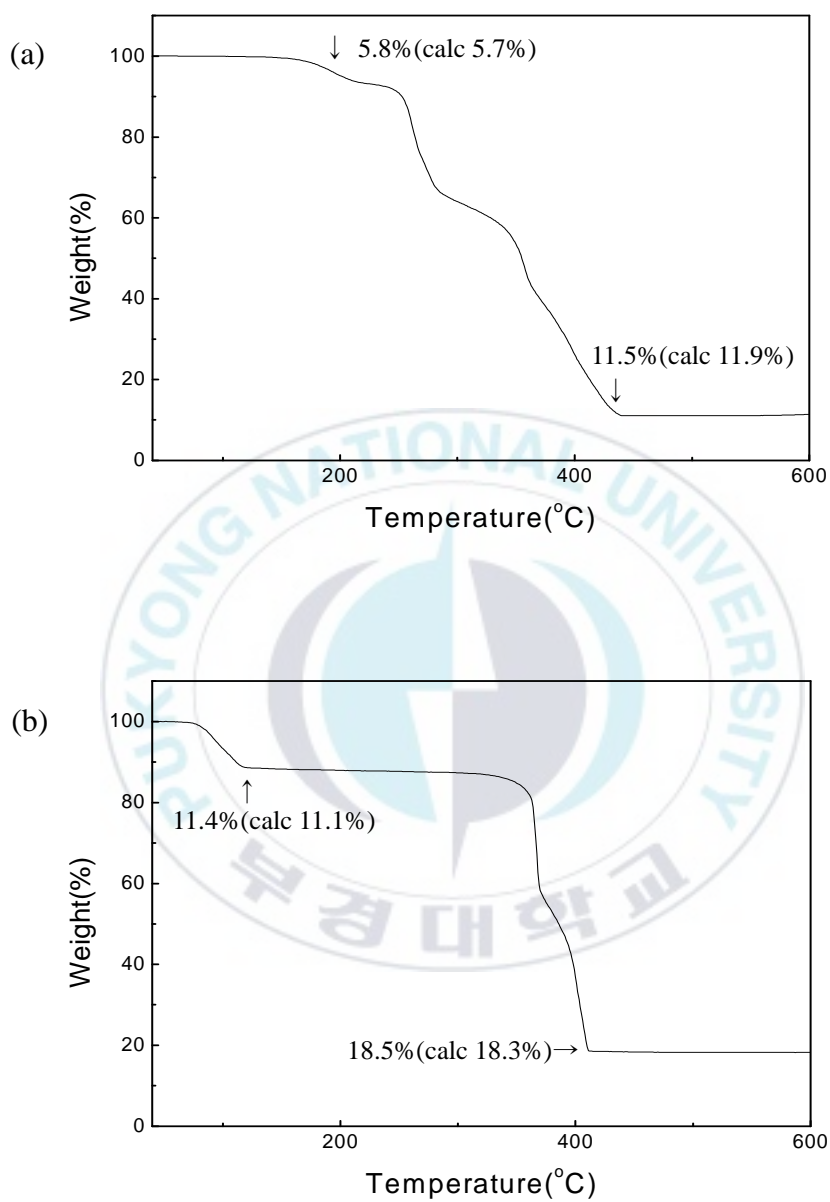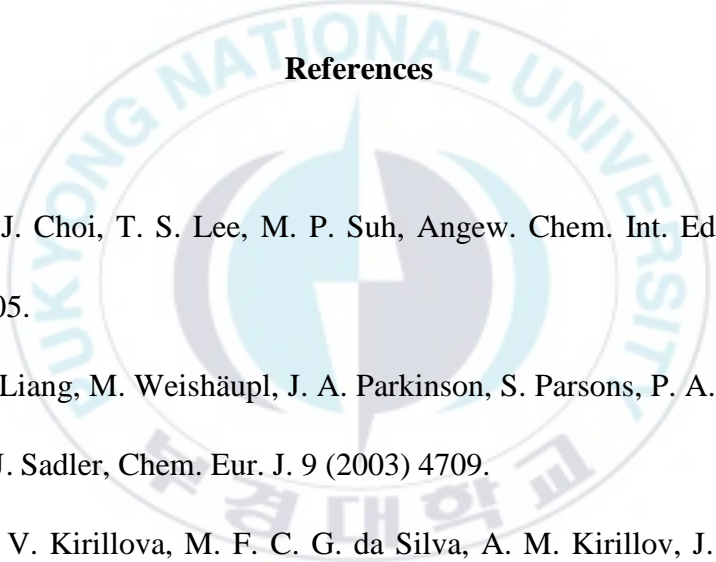
Figure 2.7. Thermogravimetric analyses of (a) [Ni(**L1**)(Hdipic)$_2$]·2H$_2$O (**1**) and (b) [Ni(**L1**)(H$_2$O)$_2$][Ni(dipic)$_2$]·2.5H$_2$O (**2**)

Supplementary material

Crystallographic data have been deposited at the Cambridge Crystallographic Data Center (CCDC), CCDC Nos. 614484 for **1** and 614485 for **2**.

References

[1]   H. J. Choi, T. S. Lee, M. P. Suh, Angew. Chem. Int. Ed. 38 (1999) 1405.

[2]   X. Liang, M. Weishäupl, J. A. Parkinson, S. Parsons, P. A. McGregor, P. J. Sadler, Chem. Eur. J. 9 (2003) 4709.

[3]   M. V. Kirillova, M. F. C. G. da Silva, A. M. Kirillov, J. J. R. F. da Silva, A. J. L. Pombeiro, Inorg. Chim. Acta 360 (2007) 506.

[4]   E. Y. Lee, M. P. Suh, Angew. Chem. Int. Ed. 43 (2004) 2798.

[5]   X. Liang, P. J. Sadler, Chem. Soc. Rev. 33 (2004) 246.

[6]   J. C. Kim, A. J. Lough, H. Park, Y. C. Kang, Inorg. Chem. Commun. 9 (2006) 514.

[7]   L. Yang, D. C. Crans, S. M. Miller, A. La Cour, O. P. Anderson, P. M.

Kaszynski, M. E. Godzala III, L. D. Austin, G. R. Willsky, Inorg. Chem. 41 (2002) 4859.

[8]   P. Buglyó, D. C. Crans, E. M. Nagy, R. L. Lindo, L. Yang, J. J. Smee, W. Jin, L.-H. Chi, M. E. Godzala III, G. R. Willsky, Inorg. Chem. 44 (2005) 5416.

[9]   O. R. Evans, W. Lin, Chem. Mater. 13 (2001) 2705.

[10]   S. Kitagawa, R. Kitaura, S.-i Noro, Angew. Chem. Int. Ed. 43 (2004) 2334.

[11]   D. L. Hoof, D. G. Tisley, R. A. Walton, J. Chem. Soc., Dalton Trans. (1973) 200.

[12]   I. Morimoto, S. Tanaka, Anal. Chem. 35 (1963) 141.

[13]   C. Sheu, D. T. Sawyer, J. Am. Chem. Soc. 112 (1990) 8212.

[14]   E. K. Barefield, A. Bianchi, E. J. Billo, P. J. Connolly, P. Paoletti, J. S. Summers, D. G. Van Derveer, Inorg. Chem. 25 (1986) 4197.

[15]   S.-G. Kang, J. K. Kweon, S.-K. Jung, Bull. Kor. Chem. Soc. 12 (1991) 483.

[16]   Z. Otwinowski, W. Minor, In Methods in Enzymology, Macromolecular Crystallography, Part A; Carter, C. W., Sweet, R. M., Eds.; Academic Press: London, 1997; Vol. 276, pp 307-326.

[17]   G. M. Sheldrick, *SHELXL\PC* V6.1 Windows NT Version; Bruker

        Analytical X-ray Systems Inc.: Madison, WI, 2001.

[18]   K.-Y. Choi, H. Ryu, Y.-M. Lim, N.-D. Sung, U.-S. Shin, M. Suh,

        Inorg. Commun. Commun. 6 (2003) 412.

[19]   Y.-H. Wen, Z.-J Li, Y.-Y. Qin, Y. Kang, Y.-B. Chen, J.-K. Cheng, Y.-

        G. Yao, Acta Cryst. E58 (2002) m762.

[20]   P. L. A. Gourdon, J.-P. Launay, Inorg. Chem. 34 (1995) 5129.

[21]   Y. Wang, M. Odoko, N. Okabe, Acta Cryst. E60 (2004) m1178.

[22]   P. L. A. Gourdon, J.-P. Launay, Inorg. Chem. 34 (1995) 5138.

[23]   P. P. Quaglieri, H. Loiseleur, G. Thomas, Acta Cryst. B28 (1972)

        2583.

[24]   M. G. B. Drew, G. W. A. Fowles, R. W. Matthews, R. A. Walton, J.

        Am. Chem. Soc. 91 (1969) 7769.

[25]   K. Mochizuki, T. Kindo, Inorg. Chem. 34 (1995) 6241.

[26]   J. C. Kim, J. Cho, H. Kim, A. J. Lough, Chem. Commun. (2004) 1796.

CHAPTER III

One-dimensional macrocyclic zinc(II) coordination polymers containing an unusual coordination of polycarboxylate ligands

Abstract

Two new zinc(II) complex of the composition $\{[Zn(\mathbf{L2})(oxalate)] \cdot 3.5H_2O\}_n$ (**1**) and $\{[Zn(\mathbf{L2})(H_2pm)] \cdot H_2O\}_n$ (**2**) (**L2** = 5,16-dimethyl-2,6,13,17-tetraazatricyclo$[16.4.0^{1.18}.0^{7.12}]$docosane, pm = pyromellitate, 1,2,4,5-benzenetetracarboxylate) have been prepared and structurally characterized by a combination of analytical, spectroscopic, thermogravimetric, and crystallographic methods. The bridging oxalate ligand in **1** shows an unusual twisted bis-monodentate coordination (1,1'-bicoordination) mode to the zinc(II) ions, resulting in the formation of an ultimate one-dimensional coordination polymer. And the complex **2** shows 1D coordination polymer containing the unusual coordination of 1,5-COO$^-$ groups in the bridging H$_2$pm ligand to zinc(II) macrocycle. These unusual structures are caused by the enhanced rigidity and steric hindrance of the macrocycle **L2** by the

introduction of *cis*-fused cyclohexane rings and methyl groups on the 14-membered tetraazamacrocycle.

Introduction

Macrocyclic transition metal complexes with polycarboxylate ligands have been proved to be good building blocks for the construction of coordination polymers and multi-dimensional supramolecular networks [1-9]. Coordination polymers are generally composed of metal ion 'connectors' and multidentate ligand 'linkers', and the dimensionality of coordination polymers can be tuned by controlling the coordination sites of metal ion 'connectors' for multidentate ligand 'linkers'[1]. Thus, the construction of one-dimensional coordination polymers is possible to be achieved by blocking equatorial sites of metal ions with polyazamacrocycles and leaving axial sites open for bridging ligands.

An oxalate ligand as a linker has allowed the construction of a number of dinuclear complexes as well as one-, two-, and three-dimensional transitional metal complexes which have potential applications in chirality, magnetism and NLO areas [10,11]. In spite of the richness of studies on such oxalato metal complexes the bis-bidentate coordination mode of the bridging oxalate ligands

to form five membered chelate rings with the central metal ions is predominant, and the number of structurally characterized bis-monodentate (1,1'-*cis*-bidentate or 1,1'-*trans*-bidentate) compounds is extremely rare [12,13]. This is especially the case for complexes in which the oxalate ligand is coordinated to metal ions by a 1,1'-*cis*-bidentate coordination mode. One good example is a polymeric copper(II) complex, $[Cu(\mu\text{-oxalate})(H_2O)(4\text{-apy})_2]_n$ (4-apy = 4-aminopyridine) [12].

Among multidentate ligand 'linkers', H_4pm is one of the attracting linkers due to its versatile coordination tendencies of carboxylic acid groups to metal ions depending on the degree of deprotonation[14-24]. Moreover, the carboxylic acid groups of H_4pm in metal complexes can act as hydrogen bond donors and/or acceptors *via* inter- and/or intramolecular fashion in extending the structures.

In this chapter, we add another example of such a complex and describe the synthesis and structure of this new one-dimensional coordination polymer $\{[Zn(\mathbf{L2})(\text{oxalate})]\cdot 3.5H_2O\}_n$ (**1**) and $\{[Zn(\mathbf{L2})(H_2pm)]\cdot H_2O\}_n$ (**2**) (see Chart 1) built by taking advantage of the rigidity, directionality and steric hindrance of the zinc(II) macrocycle 'connectors' along with the ability of oxalate and H_2pm 'linkers' to bridge between zinc(II) ions.
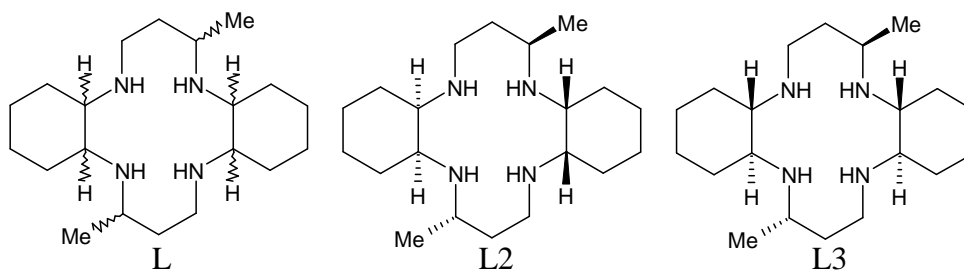
Chart 1. Illustration of macrocyclic ligands L, L2 and L3.

Experimental

Materials and Methods

All chemicals used in the synthesis were reagent grade and used without further purification. Distilled water was used for all procedures. Infrared spectra of solid samples were recorded in a Perkin-Elmer Paragon 1000 FT-IR spectrophotometer between 4000cm^{-1} and 400cm^{-1} as Nujol mulls on KBr discs. Thermal analysis (TGA-DTG) was performed on a Perkin-Elmer Model TGA-7 Thermogravimetric Analyzer under air from 50 to 800 ^{o}C at a heating rate of 10 ^{o}C/min. Elemental analysis was performed by the Korea Research Institute of Chemical Technology, Daejeon, Korea.

Synthesis of [Zn(**L2**)][NO$_3$]$_2$

The free ligand **L2** was synthesized by literature procedures [25,26]. The precursor complex [Zn(**L2**)][NO$_3$]$_2$ was prepared by refluxing ligand **L2** (3.36 g, 1.0 mmol) and Zn(NO$_3$)$_2$·6H$_2$O (3g, 1.01 mmol) in stirring methanol for a day, filtering the white powder, washing with methanol, and finally drying in air. Yield > 95%.

*Synthesis of **1***

Compound **1** was prepared by adding an aqueous solution of potassium oxalate monohydrate (184 mg, 1.0 mmol) to a DMF/H$_2$O solution of [Zn(**L2**)][NO$_3$]$_2$ (526 mg, 1.0 mmol). Slow evaporation of the solution provided colorless single crystals of **1**. Suitable crystals for X-ray diffraction studies and other measurements were manually collected under the microscope. Yield > 90%. Anal. Calcd. for C$_{22}$H$_{47}$N$_4$O$_{7.5}$Zn (**1**): C, 47.73; H, 8.50; N, 10.13%. Found: C, 47.99; H, 8.44; N, 10.07%.

Synthesis of 2

To a DMF/H_2O solution of [Zn(**L2**)][NO_3]$_2$ (526 mg, 1.0 mmol) was added a DMF solution of H_4pm (254 mg, 1.0 mmol). The mixture was allowed in an open beaker at room temperature. Colorless blocks of **2** were obtained in a week. Suitable crystals of **2** for X-ray diffraction studies and other measurements were manually collected under the microscope. Doubly deprotonated H_2pm anions were always involved in the structure of **2** even in the absence of a base. Yield > 90%. Anal. Calcd. for $C_{30}H_{46}N_4O_9Zn$(**2**): C, 53.56; H, 6.84; N, 8.33; O, 21.42%. Found: C, 53.51; H, 7.35; N, 8.76; O, 20.48 %.

X-ray crystallography

A summary of selected crystallographic data and structure refinement for **1** and **2** are given in Table 3.1. X-ray data were collected on a Nonius Kappa CCD diffractometer, using graphite monochromated Mo K$_\alpha$ radiation (λ = 0.71073 Å). A combination of 1° ϕ and ω (with κ offsets) scans were used to collect sufficient data. The data frames were integrated and scaled using the

Denzo-SMN package [27]. The structure was solved and refined using the SHELXTL\PC V6.1 package [28]. Refinement was performed by full-matrix least squares on F^2 using all data (negative intensities included). Hydrogen atoms were included in calculated positions, except for those involving hydrogen bonding specifically for the hydrogen atoms bonded to the nitrogen atoms, which were refined with isotropic thermal parameters. In the complex **2**, the crystals seemed to be twinned and/or the diffraction pattern was effected by the fact that atom Zn2 was slightly displaced from the center of symmetry causing it to be disordered. The structure contained two unique Zn atoms (Figure 3.3) for asymmetric unit and gave the predicted 1D structure. Some other residual electron density presumed water located in a void could not be resolved. The program SQUEEZE was used to remove this residual density [29]. The program suggested one molecule of water per asymmetric unit, therefore this was added to the formula.

Table 3.1. Crystal data and structure refinement for
{[Zn(**L2**)(oxalate)]·3.5H$_2$O}$_n$ (**1**) and {[Zn(**L2**)(H$_2$pm)]·H$_2$O}$_n$ (**2**)

	1	2
Empirical formula	C$_{22}$H$_{47}$N$_4$O$_{7.5}$Zn	C$_{30}$H$_{46}$N$_4$O$_9$Zn
Formula weight	553.01	672.08
Temperature (K)	150(1)	150(2)
Crystal system	Triclinic	Triclinic
Space group	P -1	P -1
a (Å)	10.6117(4)	10.7864(11)
b (Å)	11.3617(5)	12.855(2)
c (Å)	12.4952(6)	12.8584(17)
α (°)	66.468(2)	75.423(7)
β (°)	74.220(2)	67.982(8)
γ (°)	89.381(2)	70.936(9)
Volume (Å^3)	1320.98(10)	1545.2(4)
Z	2	2
D$_{calcd}$ (Mg/m^3)	1.390	1.445
Absorption coefficient	0.979 mm^{-1}	0.855 mm^{-1}
Crystal size (mm^3)	0.46 x 0.26 x 0.17	0.18 x 0.18 x 0.04
θ range for data collection	2.65-27.49°	2.59-25.13°
Index range	-13 ≤ h ≤ 12	-10 ≤ h ≤ 12
	-14 ≤ k ≤ 14	-14 ≤ k ≤ 15
	-16 ≤ l ≤ 16	-15 ≤ l ≤ 15
Reflections collected	12543	5142
Independent reflections	5820	5142
	[R(int) = 0.0616]	[R(int) = 0.117]
Goodness-of-fit on F^2	1.052	1.038
Final R indices [I>2σ(I)]	R1 = 0.0443	R1 = 0.0748
	wR2 = 0.1070	wR2 = 0.1973
R indices (all data)	R1 = 0.0743	R1 = 0.1134
	wR2 = 0.1256	wR2 = 0.2173

Results and Discussion

*Descriptions of structures for **1** and **2***

The crystal of **1** consists of a 1D coordination polymer with a basic [Zn(**L2**)(oxalate)] unit (Figs. 3.1 and 3.2). The coordination environment about the central zinc(II) ion shows a distorted octahedron in the chain direction with four Zn-N and two Zn-O bonds. The Zn-N distances are normal and vary from 2.105(2) Å to 2.135(2) Å with an average distance of ~ 2.120 Å (Table 3.2). The Zn-O distances are in the range of 2.175(17) Å - 2.2352(17) Å. These lie in the upper part of the range of values reported for related compounds ([Zn(**L3**)(apc)$_2$]; Zn-O = 2.099(2) Å [30], {Zn(**L1**)(phthalate)}$_n$·(CH$_3$OH)$_{2n}$; Zn-O = 2.220(2), 2.190(2) Å [7], {Zn(**L1**)(tp)·H$_2$O}$_n$; Zn-O = 2.1559(12) Å [31], {Zn(**L1**)(H$_2$pm)·2H$_2$O}$_n$; Zn-O = 2.2839(14) Å [31], Zn(**L1**)(H$_2$btc)$_2$·2DMF; Zn-O = 2.2222(12) Å [31], [Zn$_2$(**L1**)$_2$(oxalate)]·2ClO$_4$·2DMF; Zn-O = 2.1175(11), 2.1397(11) Å [31], {[Zn(**L1**)(maleate)$_2$·H$_2$O]}$_n$; Zn-O = 2.1968(16), 2.2840(16) Å [32]; where **L1** = 1,4,8,11-tetraazacyclotetradecane, cyclam, apc = 3-amino-2-pyrazinecarboxylate, tp = terephthalate and btc = 1,3,5-benzenetricarboxylate).

Two independent macrocycles are observed in the structure and each zinc atom sits on an inversion center. Two noteworthy features are observed in the complex **1**. One is that the complex **1** contains the interesting macrocycle **L2**, which is one out of 16 possible diastereoisomers of **L** (see Chart 1). As far as we know, the complex **1** and **2** are the first examples of a structurally characterized zinc(II) complex of the macrocyclic ligand, **L2,** which contains *cis*-fused cyclohexane rings. The cyclohexane subunits in **L2** are *anti* with respect to the plane of the macrocycle. There have been several structural reports for the transition metal complexes of **L3** containing *trans*-fused cyclohexane rings, but only three examples of nickel(II) complexes with **L2** have been prepared and structurally characterized [25,33,34]. Recent studies indicate quite different coordination behaviors and chemical properties between transition metal complexes of **L2** and **L3** [25,33]. For example, the bicarbonate ligands coordinate to the nickel(II) ion of [Ni(**L2**)][ClO$_4$]$_2$ to form a 1D supramolecule $\{[Ni(\textbf{L2})(OCO_2H)_2]\}_n$ in which the coordination environment around the nickel(II) ion is a distorted octahedron, whereas bicarbonate anions do not involve in coordination with the nickel(II) ion of [Ni(**L3**)][ClO$_4$]$_2$ [33]. They only remain as counteranions forming a hydrogen bonded supramolecule $\{[Ni(\textbf{L3})]\cdot 2HCO_3\}\}_n$, where the geometry around the

60

nickel(II) ion is a square plane. Solution chemistry also indicates that the nickel(II) complex of *cis*-fused isomer binds various solvent molecules more easily than the nickel(II) complex of *trans*-fused isomer does [25]. Although the present ligand **L2** has a close resemblance to a cyclam and its analogues, it never affords a folded structure with metal ions, but a cyclam does [31,35]. This is ascribed to the enhancement of the rigidity of the macrocycle by the introduction of cyclohexane rings in **L2**. The rigidity of the macrocycle **L2** in **1** forces the oxalate ligand to coordinate to the zinc(II) ions in a bis-monodentate mode rather than a bis-bidentate coordination mode. Another thing to note is that the bridging oxalate ligand is not planar. The two carboxylate groups in the oxalate ligand are twisted with respect to the carbon-carbon bond (C11-C22) which leads to a dihedral angle (O1-C11-C12-O4) of -74.2^o between the O1-C11-O2 and O3-C12-O4 planes. The twisted oxalate ligand bridges the zinc(II) ions using only one oxygen atom of each of its two carboxylate groups while the second one remains uncoordinated. The interatomic distances of O1-O3 = 3.195 Å and O1-O4 = 2.952 Å indicate that the oxalate ligand is best considered as coordinating to the zinc(II) ions by a 1,1'-*cis*-bidentate coordination mode. The steric hindrance of the bulky cyclohexane rings and methyl groups causes the bridging oxalate ligand to

twist so that the steric repulsions are minimized. Numerous oxalate bridged metal complexes have been reported, however, binuclear metal complexes with a planar bis-bidentate coordination mode are dominant [10,31,35-37].
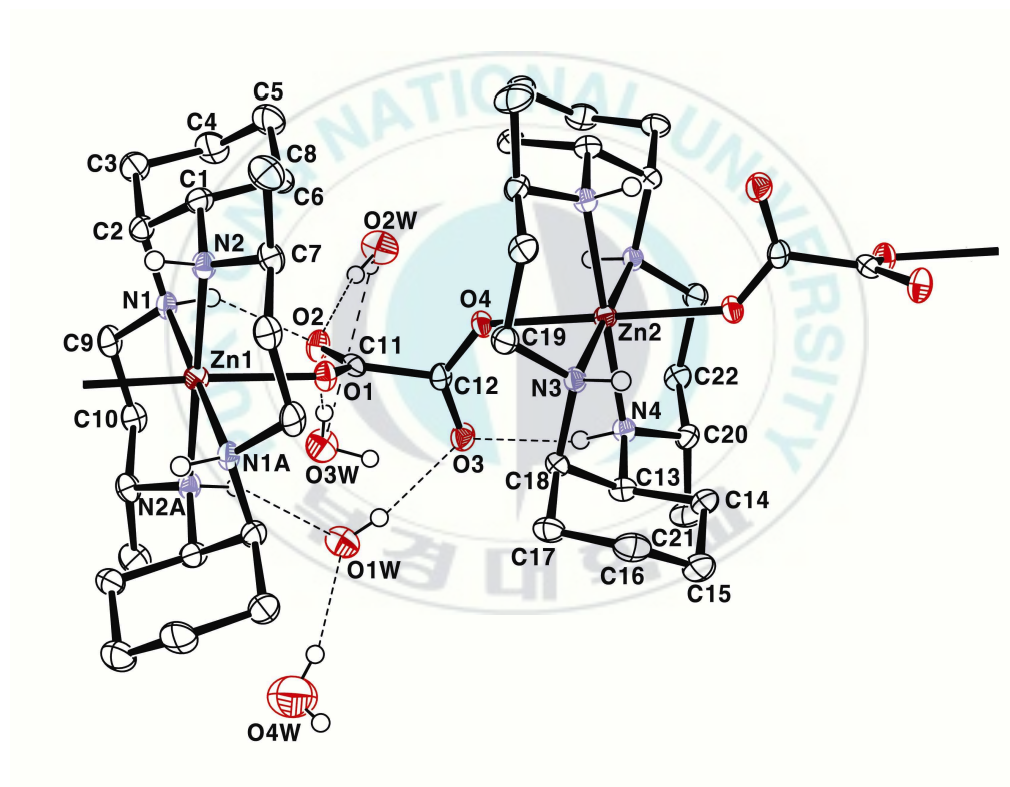
Figure 3.1. Molecular structure of $\{[Zn(\mathbf{L2})(\text{oxalate})]\cdot 3.5H_2O\}_n$ (**1**) with atom-labeling scheme. Hydrogen atoms other than those participating in hydrogen bonding are omitted for clarity.
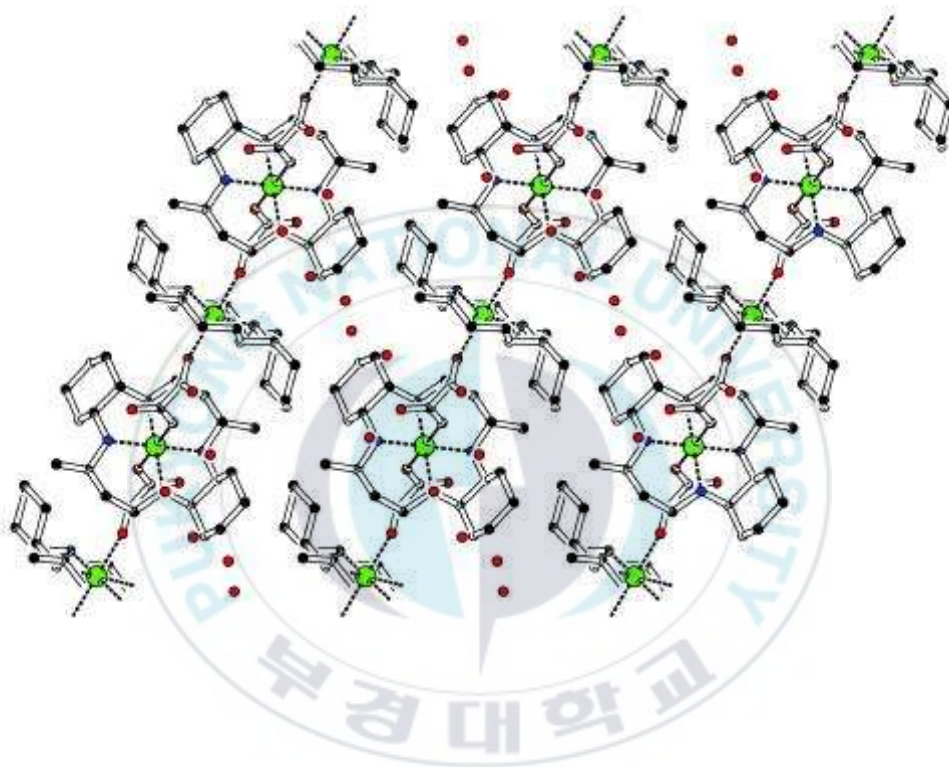
Figure 3.2. View of one-dimensional chain of $\{[Zn(\mathbf{L2})(\text{oxalate})]\cdot3.5H_2O\}_n$

(**1**) running toward crystallographic c direction.

Table 3.2. Selected bond lengths (Å) and angles (^{o}) for
{[Zn(**L2**)(oxalate)]·3.5H$_2$O}$_n$ (**1**)

Zn1-N1	2.105(2)
Zn1-N2	2.135(2)
Zn2-N3	2.119(2)
Zn2-N4	2.122(2)
Zn1-O1	2.2352(17)
Zn2-O4	2.2175(17)
N1-Zn1-N2	83.38(8)
N1-Zn1-N2#1	96.62(8)
N1-Zn1-O1	93.57(7)
N1-Zn1-O1#1	86.43(7)
N2-Zn1-O1#1	87.55(7)
N2-Zn1-O1	92.45(7)
N3-Zn2-N4	83.53(8)
N3-Zn2-O4	89.31(7)
N4-Zn2-O4	89.96(7)
N3-Zn2-N4#2	96.47(8)
N3-Zn2-O4#2	90.69(7)
N4-Zn2-O4#2	90.04(7)

Symmetry transformations used to generate equivalent atoms:

#1 -x+1,-y+1,-z+1   #2 -x+2,-y+1,-z

Table 3.3. Hydrogen bonds for $\{[Zn(\textbf{L2})(oxalate)]\cdot3.5H_2O\}_n$ (**1**) (Å and °)

D-H…A	d(D-H)	d(H…A)	d(D…A)	<(DHA)
N2-H2A...O1W#1	0.93	2.29	3.165(3)	155.8
N3-H3...O3W#3	0.93	2.19	3.077(3)	158.3
N4-H4...O3	0.93	2.11	2.967(3)	153.5
O1W-H1WA...O3	0.80(5)	2.05(5)	2.831(3)	166(5)
O1W-H1WB...O3W	0.71(4)	2.38(5)	2.994(4)	145(4)
O2W-H2WA...O2	0.87(4)	1.95(4)	2.810(3)	169(4)
O2W-H2WB...O3#4	0.83(5)	2.08(5)	2.864(3)	158(4)
O3W-H3WA...O2	0.80(5)	2.07(5)	2.846(3)	164(4)
O3W-H3WB...O2W#4	0.93(5)	1.85(5)	2.778(4)	175(4)
O4W-H4WA...O1W	0.842(5)	2.06(3)	2.882(7)	166(11)
O4W-H4WB...O1W#5	0.842(5)	2.12(3)	2.943(8)	166(13)

Symmetry transformations used to generate equivalent atoms:

#1 -x+1,-y+1,-z+1   #2 -x+2,-y+1,-z   #3 x+1,y,z

#4 -x+1,-y+1,-z   #5 -x+1,-y,-z+1

The structure of **2** exhibits the undulated 1D coordination polymer $\{[Zn(\mathbf{L2})(H_2pm)]\cdot H_2O\}_n$ with a basic $[Zn(\mathbf{L2})(H_2pm)]\cdot H_2O$ unit (Fig. 3.3). The 1D chains are linked together *via* the face-to-face π-π interactions between the aromatic rings of coordinated H_2pm ions to generate an extended supramolecular structure. The coordination environment around the central zinc(II) is a distorted octahedron with four Zn-N bonds from the macrocycle and two Zn-O bonds from the H_2pm ligands. The Zn-N distances are in the range of 2.102(4) - 2.263(5) Å (Table 3.4). The Zn-O distances of 2.207(4) and 2.170(3) Å lies within the previously reported values in related systems ($[Zn(\mathbf{L3})(apc)_2]$; Zn-O = 2.099(2) Å [30], $[Zn_2(xylyl\text{-}bicyclam)(OAc)_2](OAc)_2\cdot 2CH_3OH$; Zn-O = 2.089(2), 2.407(2) Å [38], $\{Zn(\mathbf{L1})(phthalate)\}_n\cdot(CH_3OH)_{2n}$; Zn-O = 2.220(2), 2.190(2) Å [7], $\{Zn(\mathbf{L1})(tp)\cdot H_2O\}_n$; Zn-O = 2.1559(12) Å [31], $\{Zn(\mathbf{L1})(H_2pm)\cdot 2H_2O\}_n$; Zn-O = 2.2839(14) Å [31], $Zn(\mathbf{L1})(H_2btc)_2\cdot 2DMF$; Zn-O = 2.2222(12) Å [31], $\{[Zn(\mathbf{L1})(maleate)_2\cdot H_2O]\}_n$; Zn-O = 2.1968(16), 2.2840(16) Å [32]). Two pertinent features are found in the complex **2**. One is that the complex **2** contains an interesting macrocycle **L2** like the complex **1**. Another noteworthy feature found in **2** is the unusual coordination of 1,5-COO^- groups of H_2pm to zinc(II) macrocycle. Although diverse coordination modes and shapes for

H$_4$pm, H$_3$pm, H$_2$pm, and pm moieties are understood depending on the degree

of deprotonation and the types of hydrogen bonds involved, the coordination

of 1,4-COO$^-$ groups of H$_2$pm to metal ions is dominant, and the involvement

of 1,5-COO$^-$ groups of H$_2$pm in coordination is unprecedented (Scheme 3.1).
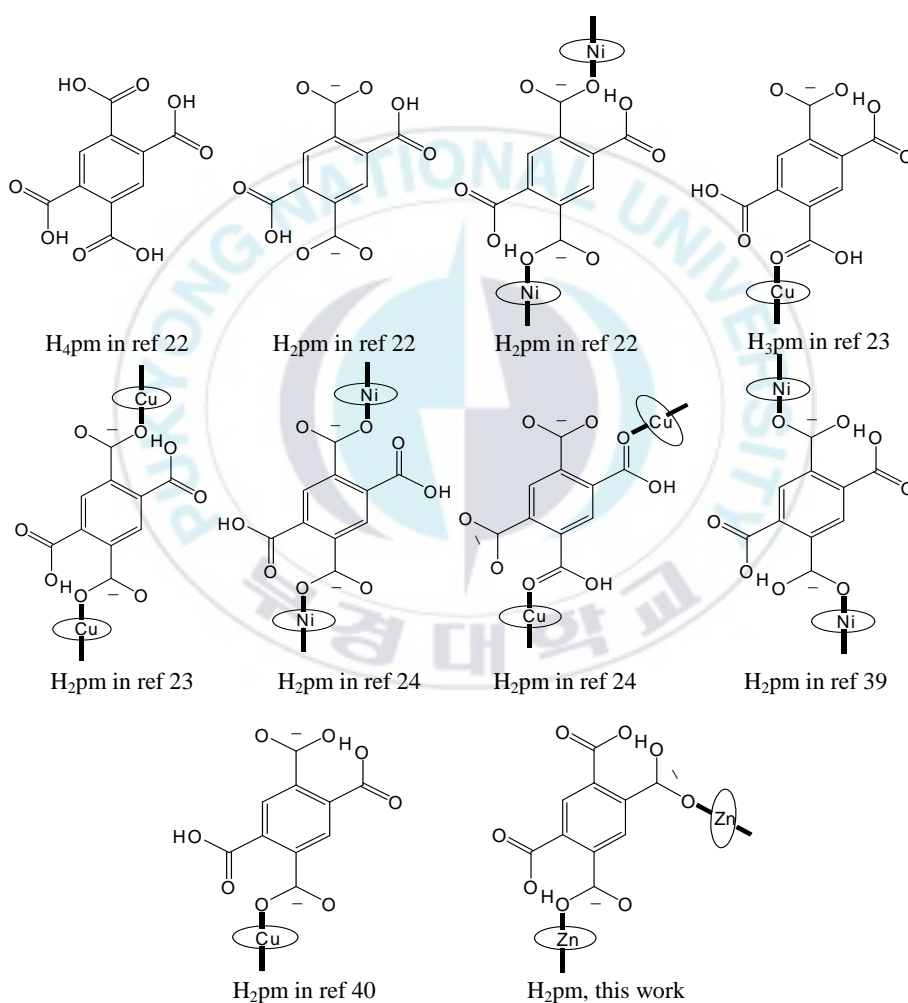

Scheme 3.1. Versatility of H$_4$pm, H$_3$pm and H$_2$pm, and their coordination and

hydrogen bonding modes.

The previously reported copper(II) complex $\{[Cu(\textbf{L1})(H_2pm)]\cdot H_2O\}_n$ may be a system to be comparable with the present complex **2**, but the 1,5-COOH groups of H_2pm rather than 1,5-COO$^-$ groups coordinate to copper(II) ions *via* their carbonyls in $\{[Cu(\textbf{L1})(H_2pm)]\cdot H_2O\}_n$ [24]. As is usual, the macrocyclic skeleton in **2** retains the *trans* III conformation with two sets of pre-organized N-H groups which enable to interact with H_2pm anions in the proface through coordination and intermolecular hydrogen bonds, contributing the formation of the coordination polymer **2**. Each COOH group on 2,4-positions is participating in an intramolecular hydrogen bond with neighboring COO$^-$ groups on 1,5-positions, respectively (Table 3.5).

In conclusion, we have prepared and fully characterized the new one-dimensional macrocyclic zinc(II) coordination polymer **1** and **2** in which the macrocyclic ligand **L2** contains *cis*-fused cyclohexane rings. The oxalate bridge in the complex **1** shows an unusual twisted bis-monodentate coordination mode to the zinc(II) ions. The bridging ligand H_2pm in the complex **2** shows the unusual coordination mode to the zinc(II) macrocycle with the involvement of 1,5-COO$^-$ rather than 1,4-COO$^-$ in coordination. We believe that this unusual structures are caused by the involvement of complex inter- and intramolecular hydrogen bonds between the zinc(II) macrocycle

'connectors' and oxalate/H_2pm 'linkers' (Fig. 3.1, 3.3 and Table 3.3, 3.5), the presence of face-to-face π-π interactions of aromatic rings between the 1D chins in the complex **2** as well as the enhanced rigidity and steric hindrance of the macrocycle **L2** by the introduction of *cis*-fused cyclohexane rings and methyl groups on the 14-membered tetraazamacrocycle.
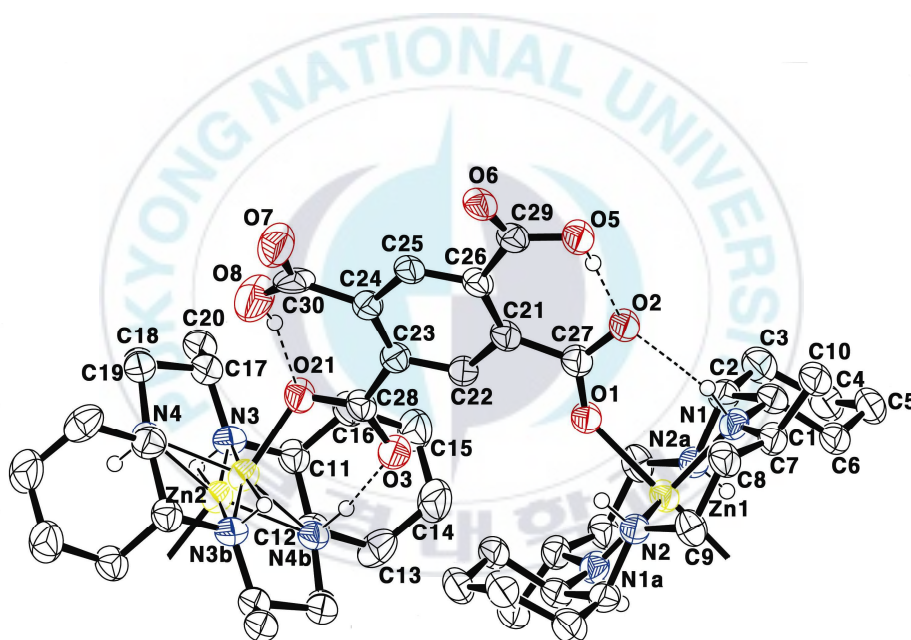
Figure 3.3. Molecular structure of {[Zn(**L2**)(H_2pm)]·H_2O}$_n$ (**2**) with atom-labeling scheme. Hydrogen atoms other than those participating in hydrogen bonding are omitted for clarity.

Table 3.4. Selected bond lengths (Å) and angles (^{o}) for {[Zn(**L2**)(H_2pm)]·H_2O}$_n$ (**2**)

Zn1-N1	2.102(4)
Zn1-N2	2.126(5)
Zn2-N3	2.263(5)
Zn2-N4	2.118(5)
Zn1-O1	2.207(4)
Zn2-O21	2.170(3)
Zn2-N3#2	2.044(5)
Zn2-N4#2	2.057(4)
N1-Zn1-N2	96.34(16)
N1-Zn1-N2#1	83.66(16)
N1-Zn1-O1	89.27(14)
N1-Zn1-O1#1	90.73(14)
N2-Zn1-O1	90.93(15)
N3-Zn2-N4	89.40(17)
N3-Zn2-O21	104.61(16)
N4-Zn2-O21	95.82(16)
N3#2-Zn2-N4	84.60(18)
N3#2-Zn2-N4#2	97.49(18)
N4#2-Zn2-N4	157.61(7)
N3#2-Zn2-O21	96.00(17)
N4#2-Zn2-O21	106.07(16)
N3-Zn2-N3#2	159.03(7)
N3-Zn2-N4#2	80.71(17)

Symmetry transformations used to generate equivalent atoms:

#1 -x+1,-y+1,-z+1   #2 -x+2,-y,-z

Table 3.5. Hydrogen bonds for $\{[Zn(\mathbf{L2})(H_2pm)]\cdot H_2O\}_n$ (**2**) (Å and °)

D-H…A	d(D-H)	d(H…A)	d(D…A)	<(DHA)
O5-H5...O2	0.84	1.59	2.406(5)	164.4
O8-H8...O21	0.84	1.65	2.432(6)	153.6
N1-H1...O2	0.93	2.08	2.970(6)	159.1
N2-H2...O7#3	0.93	2.13	3.048(6)	170.5
N3-H3...O6#4	0.93	2.52	3.370(6)	151.6
N3-H3...O21#2	0.93	2.56	3.133(6)	120.5
N4-H4...O3#2	0.93	2.01	2.897(6)	157.9

Symmetry transformations used to generate equivalent atoms:

#1 -x+1,-y+1,-z+1   #2 -x+2,-y,-z   #3 -x+1,-y+1,-z

#4 x+1,y-1,z

*Spectroscopic properties and thermal analysis of **1** and **2***

The solid state infrared spectra of **1** and **2** gave evidences for the presence of macrocyclic, oxalate and H_2pm ligands. The IR spectrum of **1** indicates νO-H bands at 3502, 3414cm^{-1}, νN-H bands at 3232, 3160cm^{-1}, ν_{as}COO band at 1568cm^{-1}, and ν_sCOO band at 1309cm^{-1}, supporting the crystal structure clearly (Fig. 3.4 (a)). The spectrum of **2** contains a νO-H band at 3425cm^{-1}, νN-H bands at 3240, 3183cm^{-1}, ν_{as}COO bands from COOH at 3145, 1709cm^{-1}, ν_{as}COO bands from COO$^-$ at 1587, 1531cm^{-1} and ν_sCOO band from COO$^-$ at 1335cm^{-1} (Fig. 3.4 (b)).

TGA-DTG curves for **1** showed a first weight loss of 11.2% (calculated 11.3%) over 35 - 88 ^{o}C with an endothermic processes centered at 80 ^{o}C, corresponding to the loss of lattice water molecules. On further heating, three consecutive weight losses were observed in 298 - 587 ^{o}C range with the loss of oxalate and macrocyclic ligands. Finally, the ZnO residue (observed 15.1%, calculated 15.3%) was remained above 587 ^{o}C (Fig. 3.5).

72
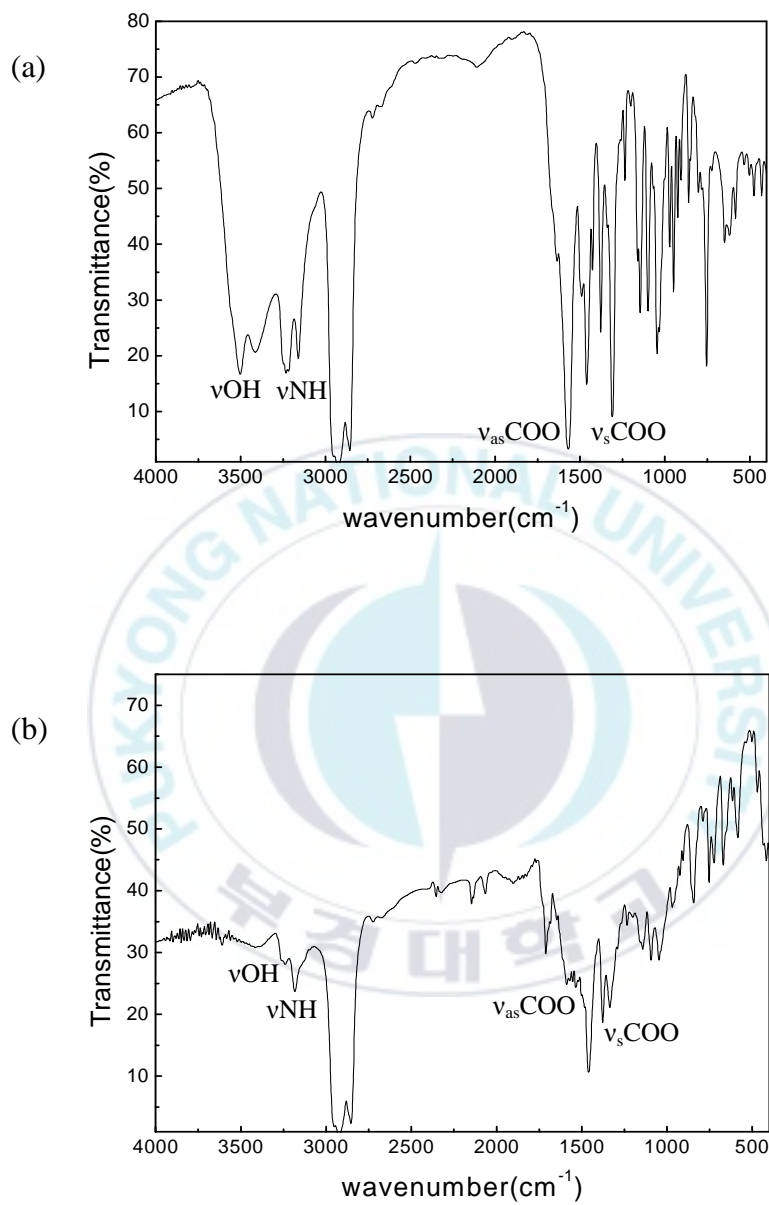
Figure 3.4. Infrared spectra of (a) $\{[Zn(\mathbf{L2})(oxalate)]\cdot 3.5H_2O\}_n$ (**1**) and (b) $\{[Zn(\mathbf{L2})(H_2pm)]\cdot H_2O\}_n$ (**2**) [Nujol mull]
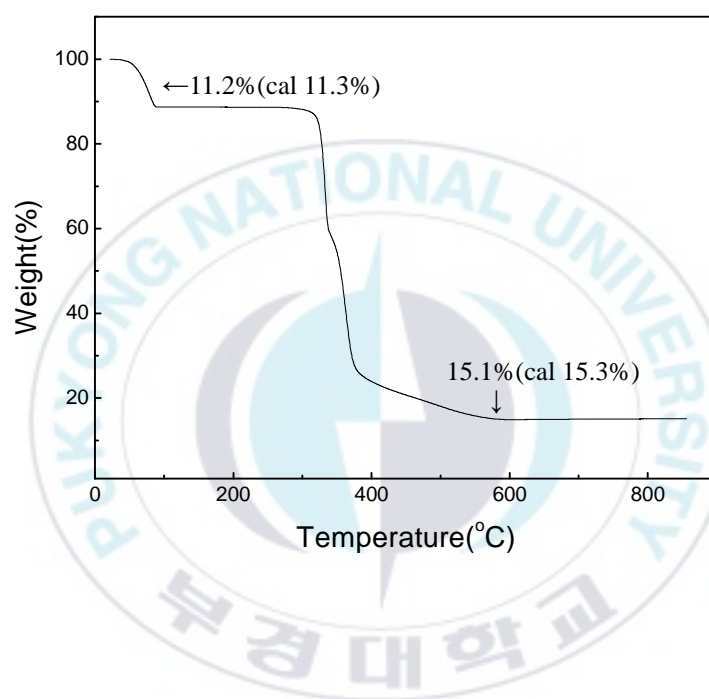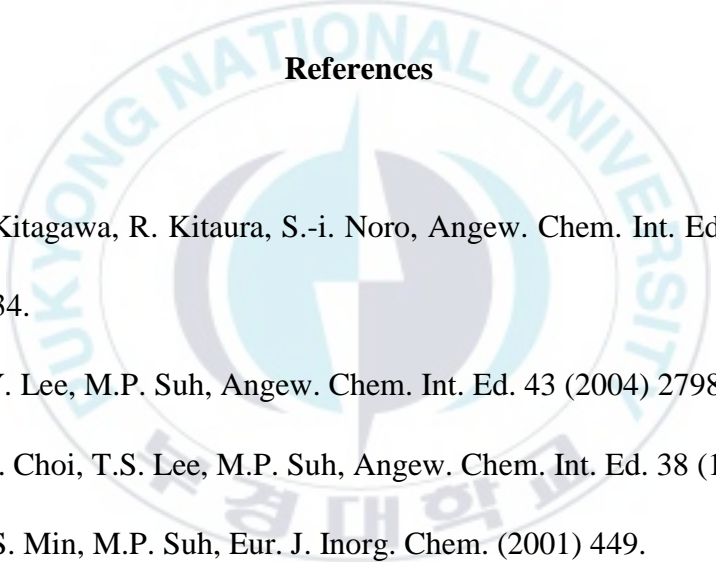
Figure 3.5. Thermogravimetric analysis of {[Zn(**L2**)(oxalate)]·3.5H$_2$O}$_n$ (**1**)

Supplementary material

Crystallographic data have been deposited at the Cambridge Crystallographic Data Center (CCDC), CCDC Nos. 622147 for **1** and 623391 for **2**.

References

[1]   S. Kitagawa, R. Kitaura, S.-i. Noro, Angew. Chem. Int. Ed. 43 (2004) 2334.

[2]   E.Y. Lee, M.P. Suh, Angew. Chem. Int. Ed. 43 (2004) 2798.

[3]   H.J. Choi, T.S. Lee, M.P. Suh, Angew. Chem. Int. Ed. 38 (1999) 1405.

[4]   K.S. Min, M.P. Suh, Eur. J. Inorg. Chem. (2001) 449.

[5]   K.S. Min, M.P. Suh, Chem. Eur. J. 7 (2001) 303.

[6]   H.J. Choi, M.P. Suh, J. Am. Chem. Soc. 120 (1998) 10622.

[7]   X. Liang, M. Weishäupl, J.A. Parkinson, S. Parsons, P.A. McGregor, P.J. Sadler, Chem. Eur. J. 9 (2003) 4709.

[8]   T.-B. Lu, H. Xiang, R.L. Luck, Z.-W. Mao, D. Wang, C. Chen, L.-N. Ji, Cryst. Eng. Chem 3 (2001) 168.

[9]   K.-Y. Choi, H. Ryu, Y.-M. Lim, N.-D. Sung, U.-S. Shin, M. Suh, Inorg. Chem. Commun. 6 (2003) 412.

[10]   M. Hernández-Molina, P. Lorenzo-Luis, C. Ruiz-Pérez, Chem. Cryst. Comm 3 (2001) 60.

[11]   C. Janiak, Dalton Trans. (2003) 2781.

[12]   O. Castillo, A. Luque, J. Sertucha, P. Román, F. Lloret, Inorg. Chem. 39 (2000) 6142.

[13]   J.C. Kim, J. Cho, A.J. Lough, Inorg. Chim. Acta 317 (2001) 252.

[14]   C.N.R. Rao, S. Natarajan, R. Vaidhyannathan, Angew. Chem. Int. Ed. 43 (2004) 1466.

[15]   H. Kumagai, C.J. Kepert, M. Kurmoo, Inorg. Chem. 41 (2002) 3410.

[16]   D. Cheng, M.A. Khan, R.P. Houser, Crystal Growth & Design 2 (2002) 415.

[17]   Q. Shi, R. Cao, D.-F. Sun, M.-C. Hong, Y.-C. Liang, Polyhedron 20 (2001) 3287.

[18]   F.D. Rochon, G. Massarweh, Inorg. Chim. Acta 304 (2000) 190.

[19]   F.D. Rochon, G. Massarweh, Inorg. Chim. Acta 314 (2001) 163.

[20]   S.V. Ganesan, S. Natarajan, Inorg. Chem. 43 (2004) 198.

[21]   R. Diniz, H.A. de Abreu, W.B. de Almeida, M.T.C. Sansiviero, N.G.

Fernandes, Eur. J. Inorg. Chem. (2002) 1115.

[22]   J.C. Kim, A.J. Lough, H. Kim, Inorg. Chem. Commun. 5 (2002) 771.

[23]   J. Cho, A.J. Lough, J.C. Kim, Inorg. Chim. Acta 342 (2003) 305.

[24]   J.C. Kim, H. Jo, A.J. Lough, J. Cho, U. Lee, S.Y. Pyun, Inorg. Chem.
        Commun. 6 (2003) 474.

[25]   S.-G. Kang, J.H. Jeong, Bull. Korean Chem. Soc. 24 (2003) 393.

[26]   S.-G. Kang, J.K. Kweon, S.-K. Jung, Bull. Korean Chem. Soc. 12
        (1991) 483.

[27]   Z. Otwinowski, W. Minor, In Methods in Enzymology,
        Macromolecular Crystallography, Part A; C.W. Carter, R.M. Sweet,
        Eds.; Academic Press: London, 1997; Vol. 276, pp 307-326.

[28]   G.M. Sheldrick, SHELXTL\PC V6.1, Bruker Analytical X-ray
        Systems, Madison, WI, 2001.

[29]   A.L. Spek, (2005) *PLATON, A Multipurpose Crystallographic Tool*,
        Utrecht University, Utrecht, The Netherlands.

[30]   H. Park, J.C. Kim, A.J. Lough, B.M. Lee, Bull. Korean Chem. Soc. 27
        (2006) 1500.

[31]   H. Jo, A.J. Lough, J.C. Kim, Inorg. Chim. Acta 358 (2005) 1274.

[32]   J.C. Kim, A.J. Lough, H. Park. Y.C. Kang, Inorg. Chem. Commun. 9

(2006) 514.

[33] J.C. Kim, J. Cho, H. Kim, A.J. Lough, Chem. Commun. (2004) 1796.

[34] J. Cho, U. Lee, J.C. Kim, Transition Met. Chem. 27 (2002) 429.

[35] L.P. Battaglia, A. Bianchi, A.B. Corradi, E. Garcia-España, M. Micheloni, M. Julve, Inorg. Chem. 27 (1988) 4174.

[36] U. García-Couceiro, D. Olea, O. Castillo, A. Luque, P. Román, P.J. de Pablo, J. Gómez-Herrero, F. Zamora, Inorg. Chem. 44 (2005) 8343.

[37] P. Vitoria, I. Muga, J.M. Gutiérrez-Zorrilla, A. Luque, P. Román, L. Lezama, F.J. Zúniga, J.I. Beitia, Inorg. Chem. 42 (2003) 960.

[38] X. Liang, J.A. Parkinson, M. Weishäupl, R.O. Gould, S.J. Paisey, H. Park, T.M. Hunter, C.A. Blindauer, S. Parsons, P.J. Sadler, J. Am. Chem. Soc. 124 (2002) 9105.

[39] J.C. Kim, J.A. Kim, Y.C. Kang, A.J. Lough, B.M. Lee, Transition Met. Chem. 31 (2006) 829.

[40] J.C. Kim, A.J. Lough, H. Jo, Inorg. Chem. Commun. 5 (2002) 616.

Acknowledgments

friends, D.Y. Kim and Jiyeon Park. Finally, I am greatly thankful to my parents

for their constant supports and thoughtfulness throughout my whole life.